https://doi.org/10.5194/egusphere-2025-1165
Preprint. Discussion started: 25 March 2025

Constraining a Radiative Transfer Model with Satellite Retrievals: Implications for Cirrus Cloud Thinning

Ehsan Erfani[1] and David L. Mitchell[1]

[1] Division of Atmospheric Sciences, Desert Research Institute, Reno, Nevada, USA

Correspondence to: Ehsan Erfani, (Ehsan.Erfani@dri.edu)

Abstract

The complex mechanisms governing the formation of cirrus clouds pose significant challenges in the accurate simulation of cirrus clouds within climate models, leading to uncertainties in predicting the cirrus cloud response to aerosols and efficacy of cirrus cloud thinning (CCT), a *climate intervention* method. One issue is related to the relative contributions of homogeneous and heterogeneous ice nucleation. Recent satellite observations from the Cloud-Aerosol Lidar and Infrared Pathfinder Satellite Observation (CALIPSO) suggest that cirrus clouds strongly affected by homogeneous ice nucleation (i.e., homogeneous cirrus) play a more important role than previously assumed. This study employs a radiative transfer model to quantify the cloud radiative effect for homogeneous and heterogeneous cirrus clouds at the top of the atmosphere (TOA), the Earth's surface, and within the atmosphere. The experiments are conducted using cirrus ice water content and effective diameter vertical profiles from CALIPSO retrievals for homogeneous and heterogeneous cirrus clouds across different regions (Arctic, Antarctic, and midlatitude) and surface types (ocean and land). Results indicate that homogeneous cirrus clouds exhibit stronger radiative effects than heterogeneous cirrus, implying that transitioning from homogeneous to heterogeneous cirrus, as an indicator of CCT efficacy, could induce substantial surface cooling, particularly in polar regions during winter. Estimated instantaneous surface cooling effects range from -0.7 to -1.0 W m^{-2}, with the TOA cooling reaching up to -1.6 W m^{-2}. This study highlights the need for improved representation of homogeneous cirrus in models to better predict the climatic impacts of cirrus clouds and to assess the CCT viability.

https://doi.org/10.5194/egusphere-2025-1165
Preprint. Discussion started: 25 March 2025

1 Introduction

Cirrus clouds are a critical component of the Earth's radiation budget; the global annual mean coverage of these clouds ranges from 17-20% (Matus and L'Ecuyer, 2017; Sassen et al., 2009) to 35% (Hong et al., 2016) with high spatial variability. Cirrus cloud coverage is about 30% in mid-latitudes and about 60-80% in the tropics (Guignard et al., 2012; Stubenrauch et al., 2006). In addition, cirrus clouds are more frequent during the winter seasons in the mid and high latitudes (Mitchell et al., 2018; Zhu et al., 2024). They significantly absorb and scatter incoming solar radiation and absorb outgoing thermal radiation from the Earth's surface and low-level clouds. Although these two effect counteract each other, it is estimated that on global annual averages, these clouds warm the planet by approximately 5 W m^{-2} (Gasparini and Lohmann, 2016). Despite their significant impacts on radiation and climate, uncertainty exists in measuring, retrieving, and modeling cirrus clouds partly because the processes involved in their formation are poorly understood (Heymsfield et al., 2017) or are not represented in climate models (Lyu and Liu, 2023). This complexity has left many important questions unanswered (Kärcher, 2017; Kay et al., 2012). In particular, our understanding of the mechanisms of cirrus cloud development and their microphysical properties, such as ice crystal shape and size distribution remain insufficient (Krämer et al., 2016; Lawson et al., 2019). Cirrus clouds exhibit diverse geometric features (Fig. 1), which reflect their varied microphysical and macrophysical properties.

One of the main uncertainties in modeling cirrus clouds is related to insufficient knowledge of the relative contribution of homogeneous and heterogeneous ice nucleations in cirrus clouds (Heymsfield et al., 2017). Homogeneous ice nucleation happens when liquid solution droplets (haze or cloud droplets) freeze spontaneously, with no ice nucleating particles (INPs) to initiate freezing. This is when the temperature (T) is colder than -38 °C and supersaturation (quantified by relative humidity with respect to ice or RH_i) is greater than 140-150%. In contrast, heterogeneous ice nucleation requires INPs to initiate freezing at warmer T and lower RH_i values (Heymsfield et al., 2017; Kanji et al., 2017). Since INP concentrations are generally much lower than solution droplet concentrations, heterogeneous cirrus usually have fewer and larger ice particles, and therefore are optically thinner, whereas homogeneous cirrus generally contain higher ice particle concentrations of smaller size, and are optically thicker (Krämer et al., 2016). With such distinct

https://doi.org/10.5194/egusphere-2025-1165
Preprint. Discussion started: 25 March 2025

microphysical properties, these two types of cirrus clouds demonstrate significantly different radiative effects, and this makes it crucial to investigate their contributions.

There are different methods to retrieve cirrus cloud properties using satellite instruments such as infrared radiometers (Magurno et al., 2020; Mitchell et al., 2018; Nazaryan et al., 2008; Stubenrauch et al., 2008; Yue et al., 2020), visible radiometers (Gao et al., 2002; Wang et al., 2019), microwave radiometers (Evans et al., 2012; Jiang et al., 2019; Wu et al., 2014), and a combination of instruments (Yorks et al., 2023). Satellite microwave radiometers have been used widely to retrieve cirrus clouds, however, their coarse spatial (Wang et al., 2001) and temporal (Jiang et al., 2019) resolutions, the sensitivity of the retrievals to surface reflectivity (Wang et al., 2001), and the need for ancillary information from the surface to properly estimate the surface albedo (Jiang et al., 2019) limit their ability for studying the cirrus clouds. Visible retrievals also have limitations such as low sensitivity to detecting cirrus clouds (especially, thin ones since they have low reflectivity and absorption in the visible range) and contamination of land surface reflectance (Schläpfer et al., 2020). On the other hand, infrared retrievals have a much lower sensitivity to surface reflectivity and can detect thin cirrus clouds using water vapor absorption bands (Roskovensky and Liou, 2003).

Figure 1. Left: Photography of sky over Reno, Nevada, USA on 25 Sep. 2023, showing cirrus clouds with various geometric features (e.g., thin and thick) (Photo taken by Ehsan Erfani). Right: Satellite imagery showing the same types of cirrus on the same day. Reno is located between Lake Tahoe and Pyramid Lake and is covered by clouds. Note that the two photos do not correspond to the same time, but provide general cloud patterns on the same day (the satellite image provided by MODIS instrument onboard NASA Terra satellite and taken from NASA Worldview website: https://worldview.earthdata.nasa.gov/).

https://doi.org/10.5194/egusphere-2025-1165
Preprint. Discussion started: 25 March 2025

The Cloud-Aerosol Lidar and Infrared Pathfinder Satellite Observations (CALIPSO) dataset has been used to study cirrus cloud properties (Li and Groß, 2021; Sassen et al., 2009). It also has some limitations; for instance, lidar-radar (DARDAR) retrievals of the ice particle number concentration (N_i) are based on assumptions about the shape of the ice particle size distribution, which can lead to uncertainties in the retrieved values (Sourdeval et al., 2018). Despite this, the CALIPSO dataset remains a valuable tool for studying cirrus clouds and their radiative impacts on climate. Recently, Mitchell and Garnier (2024) expanded on Mitchell et al. (2024) work and developed a CALIPSO retrieval to quantify homogeneous and heterogeneous cirrus on a global scale (note that the accurate terms would be "dominated by homogeneous" and "dominated by heterogeneous" ice nucleation regimes, but for simplicity, we use the terms homogeneous and heterogeneous in this study). The data from two Infrared Imaging Radiometer (IIR) channels, 12 μm and 10.6 μm, were used to calculate ice optical and microphysical properties, such as N_i, IWC, D_e, and shortwave extinction coefficient (α_{ext}) using ice particle mass-dimension and area-dimension relationships from Erfani and Mitchell (2016). To establish a threshold transition between homogeneous and heterogeneous cirrus regimes (henceforth, referred to as cirrus regimes), they considered the D_e maximum in the α_{ext} - D_e plane as this threshold (note that high N_i should limit ice particle growth and D_e due to increased competition for water vapor). In particular, they showed that although heterogeneous cirrus is dominant in most regions and seasons, the homogeneous fraction weighted by cloud optical depth contributes more than 50% during the winter in the extratropics.

The findings by Mitchell and Garnier (2024) have important implications for a *climate intervention* technique called *cirrus cloud thinning* (CCT). Climate change has disastrous effects on humans, the environment, and society, and such effects exacerbate as global CO_2 level and sea surface temperature (SST) increase (IPCC report, 2021). The last time with CO_2 concentration near 400 ppm was during the mid-Pliocene (3.25 million years ago) when global SST was 4.1°C warmer than preindustrial period (Tierney et al., 2025). Global climate models (GCMs) project that global warming will continue in the next decades (IPCC report, 2021), and even in the unlikely scenario where global greenhouse gas (GHG) emissions are eliminated by 2050 (Forster et al., 2021; Hansen et al., 2023; 2025), the global mean temperature would remain around its 2050 value for centuries unless atmospheric GHG concentrations were decreased somehow. This has prompted

https://doi.org/10.5194/egusphere-2025-1165
Preprint. Discussion started: 25 March 2025

some to advocate for a threefold solution: (1) GHG emission reductions, (2) GHG concentration reduction, and (3) climate interventions to cool the planet (Baiman et al., 2024). Solution (3) would take only several years to act, whereas solutions (1) and (2) would take several decades and thus risk triggering tipping points in the climate system (e.g., Steffen et al., 2018). Therefore, various climate intervention methods, including CCT (e.g., Gasparini and Lohmann, 2016; Mitchell and Finnegan, 2009), have been proposed to cool the planet (NASEM report, 2021). It is important to conduct comprehensive research on climate intervention methods in order to quantify their efficacy, cost, risks, and limitations. Climate intervention methods, if proven effective, are not replacements for but rather complement GHG emission reduction and removal.

CCT is a proposed climate intervention method often considered under the Solar Radiation Modification (SRM) category and is suggested to deliberately slow down the warming of the planet by injecting proper aerosols that act as ice nuclei particles (INPs) in the upper troposphere to reduce the thickness and coverage of cirrus clouds (Mitchell and Finnegan, 2009). CCT can be efficient and cool the planet if the homogeneous cirrus is abundant, leading to a transition from homogeneous to heterogeneous cirrus. Heterogeneous cirrus is considered to be dominant globally (Cziczo et al., 2013; Froyd et al., 2022), but recent satellite retrievals (Gryspeerdt et al., 2018; Mitchell et al., 2018; Mitchell and Garnier, 2024) have shown that homogeneous cirrus might have been underestimated. The effectiveness of CCT might surpass previous estimates, considering that the cooling efficacy of CCT depends on the fraction of homogeneous cirrus. CCT is most impactful in the mid- and high-latitudes during the colder months because the cirrus longwave (LW) cloud radiative effect (CRE) is significantly stronger than shortwave (SW) CRE, and therefore significant surface cooling could happen. Efficient CCT has the potential to reduce the thawing of Arctic permafrost and enhance the sea ice cover (Storelvmo et al., 2014), and thus enhance the Atlantic Meridional Overturning Current (AMOC) by cooling sea surface temperatures to promote downwelling just south of Greenland. Note that the AMOC is a climate tipping point (Steffen et al., 2018). Moreover, CCT could slow down Arctic amplification (AA), a phenomenon characterized by warming of the Arctic at a rate two to three times faster than the rest of the globe mainly because of sea ice loss (Screen and Simmonds, 2010).

Despite the cooling potential of CCT from theory (e.g., Mitchell and Finnegan, 2009), the results of modeling studies on CCT are not conclusive as some CCT simulations indicated that CCT

https://doi.org/10.5194/egusphere-2025-1165
Preprint. Discussion started: 25 March 2025

cooling is negligible (Gasparini & Lohmann, 2016; Penner et al., 2015; Tully et al., 2022) while others (Gruber et al., 2019; Storelvmo et al., 2013, 2014) showed that such cooling is significant. GCMs and regional climate models (RCMs) have significant uncertainties in predicting the microphysical properties of cirrus clouds largely because of limitations in capturing the complicated set of under-resolved physical mechanisms associated with cirrus clouds and their interactions with aerosols (Eliasson et al., 2011; Kay et al., 2012). Some possible ways for improving the treatment of CCT in GCMs are described in Mitchell and Garnier (2024). For this reason, it is important to constrain models with observations to achieve a better understanding of cirrus clouds in general and CCT in particular.

To evaluate CCT's cooling potential without the use of climate models, a radiative transfer model (RTM) is employed in this study. Over the past decades, RTMs have been used extensively to study the radiative properties of cirrus, contrail, and mixed-phase clouds, since RTMs are the most accurate tools for understanding the interaction between ice cloud properties and wavelength-dependent radiation flux in a way that is difficult to conduct in a complex GCM. RTMs have been used to determine heating rates and/or the radiative effect of ice clouds, with their microphysical characteristics sometimes measured during aircraft field campaigns (Marsing et al., 2023), retrieved from satellite measurements (Hong et al., 2016; Sun et al., 2011), or simulated by models such as stochastic cloud generators (Fauchez et al., 2017; Zhou et al., 2017) or a mesoscale cloud model complex (Khvorostyanov and Sassen, 1998). RTM simulations of cirrus clouds show that their radiative effects are highly sensitive to cloud microphysical characteristics such as ice water path (Córdoba-Jabonero et al., 2020; Fu and Liou, 1993), and ice particle shape and size (Macke et al., 1998; Takano et al., 1992; Zhang et al., 1999). A few studies (e.g., Schumann et al., 2012; Wolf et al., 2023) considered multiple microphysical and environmental parameters (e.g., temperature, surface albedo, zenith angle) when computing the radiative effect of cirrus and contrails. Despite significant progress in calculating cirrus cloud radiative properties by using an RTM, the contribution of homogeneous and heterogeneous cirrus to the total cirrus CRE and the efficacy of CCT has not been studied yet.

This study aims to combine new advances in satellite remote sensing and radiative transfer modeling to develop a conceptual platform for studying different types of cirrus clouds and their impact on Earth's energy budget. We use the novel CALIPSO satellite retrievals from Mitchell et

https://doi.org/10.5194/egusphere-2025-1165
Preprint. Discussion started: 25 March 2025

al. (2024) to infer the microphysical properties of cirrus clouds and then employ those as inputs to an RTM to calculate cirrus CREs. This is done by calculating the vertical profiles of IWC and D_e for two types of cirrus clouds (homogeneous and heterogeneous) and different environmental conditions (latitude bands, surface types, seasons) based on CALIPSO retrievals. These are then used in an RTM to calculate cirrus cloud CRE at the surface (Sfc), at top of the atmosphere (TOA), and in the column of atmosphere (Atm). By investigating the difference in CRE between homogeneous and heterogeneous cirrus, this study provides an estimate of the efficacy of CCT as a first estimate, with implications for improving GCMs. The rest of this paper is organized as follows: in Section 2, a description of the observational data and RTM experimental design is presented; the main RTM results are explained in Section 3 for relevant geographical conditions; the sensitivity to thermodynamic profiles, low clouds, and aerosols are explored in Section 4; suggestions for improving cirrus cloud modeling of CCT is provided in Section 5; and finally, conclusions are presented in Section 6.

2 Methodology

2.1 Data

The RTM requires the vertical profiles of atmospheric variables and trace gases as inputs and by default, uses available standard profiles for the tropics, mid-latitude, sub-arctic, and U.S. regions for winter and summer seasons and from surface to 120 km provided by Air Force Geophysical Laboratory (AFGL) atmospheric constituent dataset (Anderson et al., 1986). The radiative impacts of trace gases are small, so we use the standard vertical profiles of trace gases. However, the cirrus cloud properties are closely related to thermodynamic profiles, in particular temperature (T). Therefore, to force the RTM with realistic thermodynamic profiles, we replace the standard vertical profiles of T and water vapor mixing ratio (q_v) with those extracted from Modern-Era Retrospective Analysis for Research and Applications, version two (MERRA2; Gelaro et al., 2017) reanalysis dataset with a spatial resolution of 0.5×0.625°, 72 vertical levels, and a temporal resolution of 1 month. Using this dataset is preferred because it was also used in the CALIPSO satellite retrievals of homogeneous and heterogeneous cirrus clouds. The RTM requires air density

https://doi.org/10.5194/egusphere-2025-1165
Preprint. Discussion started: 25 March 2025

(ρ_a) to be consistent with thermodynamic profiles, therefore, we calculate ρ_a based on MERRA2 T and pressure (P) following the ideal gas law: $\rho_a = P/kT$, where k is Boltzmann constant. This new ρ_a is then replaced with the default ρ_a. The area-weighted averages of T, q_v, and ρ_a profiles are calculated for grid points in the Arctic (60-90°N), Antarctic (90-60°S), and the Northern Hemisphere (NH) mid-latitude (30-60°N), and for winter seasons of the same years as the CALIPSO retrievals (2008, 2010, 2012, and 2013). In addition, maximum and minimum profiles in each region are calculated as a range of change in thermodynamic variables (Fig. 2). Using RTM standard sub-arctic profiles are not justified, because they over-estimate the cold and dry profiles over the Arctic.

The CALIPSO satellite retrievals based on the methodology of Mitchell et al. (2024) and Mitchell and Garnier (2024) are used to create cirrus cloud property statistics (e.g., median and 25th and 75th percentiles) for each season, latitude band, and surface type (land or ocean). In addition, the data is grouped into homogeneous and heterogeneous cirrus categories, based on temperature-dependent α_{ext} thresholds derived from D_e maxima (related to the α_{ext}) as established by those

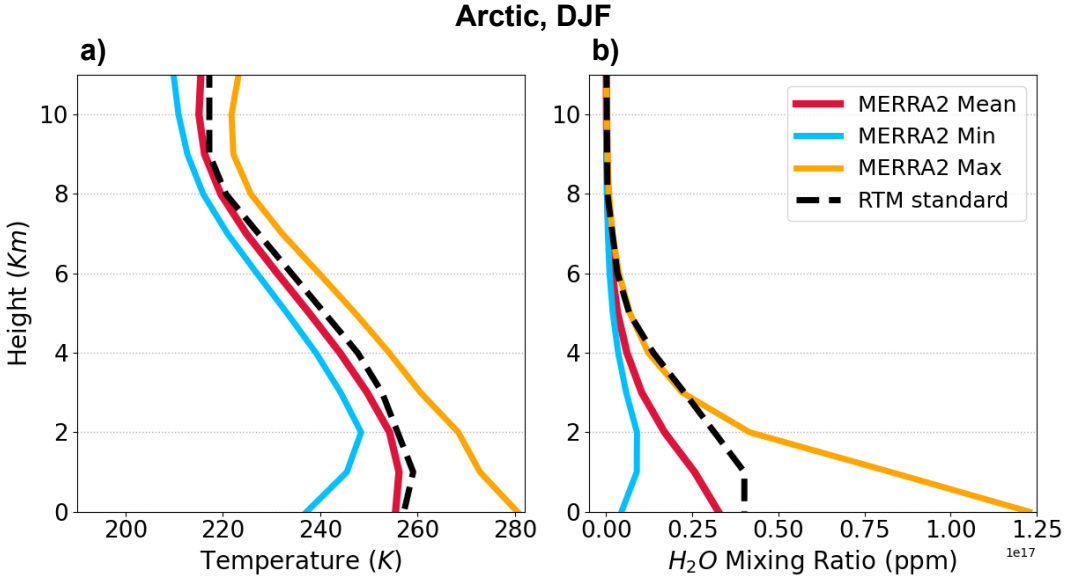

Figure 2. Vertical profiles of a) temperature and b) water mixing ratio for wintertime. The libRadtran RTM standard profiles are for subarctic (no Arctic/Antarctic profile provided), whereas MERRA2 profiles are for the Arctic region (60-90°N) during the boreal winter of 2008, 2010, 2012, and 2013. Mean refers to area-weighted average over all grid points in this region.

https://doi.org/10.5194/egusphere-2025-1165
Preprint. Discussion started: 25 March 2025

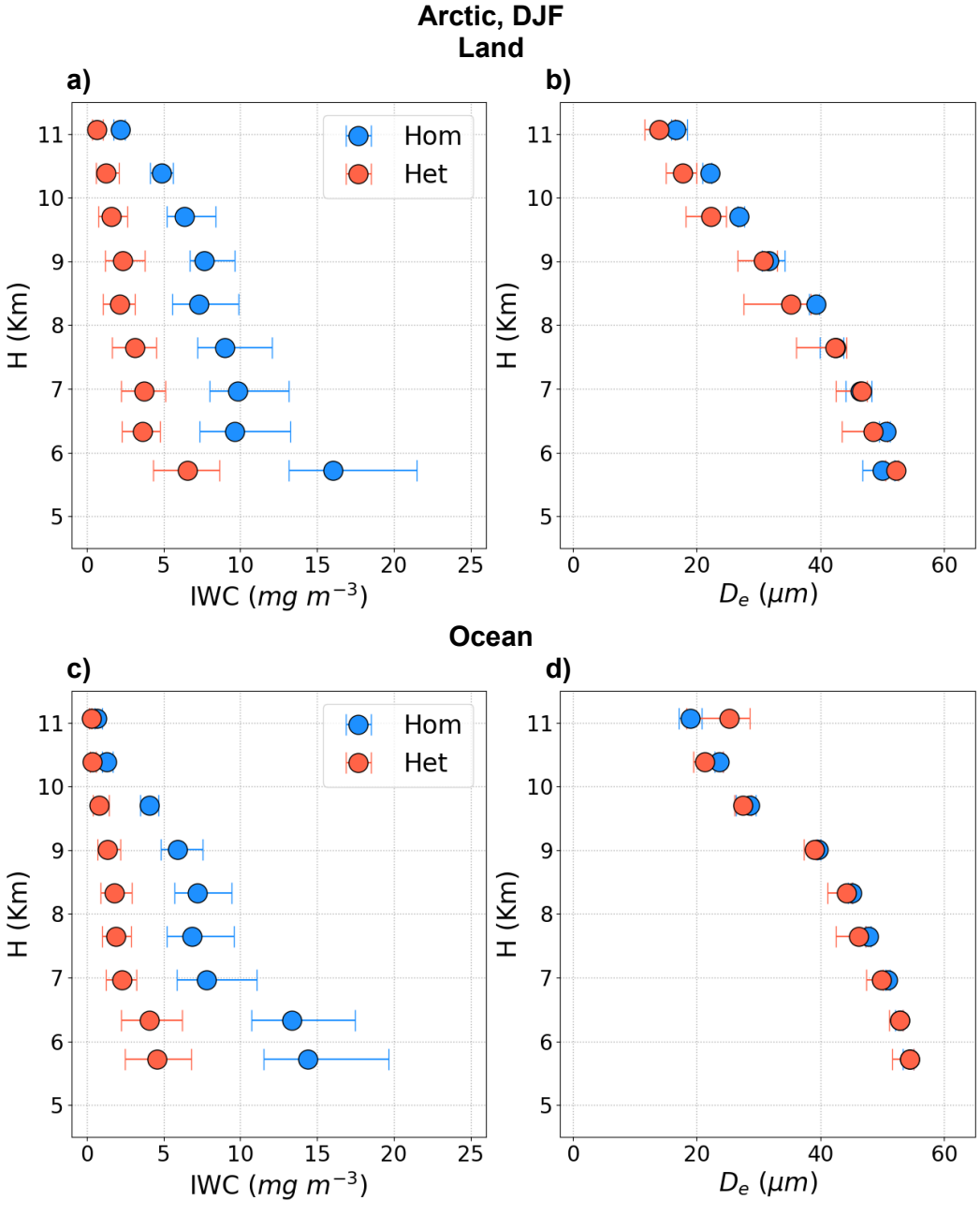

Figure 3. Microphysical properties of cirrus clouds from CALIPSO retrievals: a&c) IWC vs. height and b&d) D_e vs. height for two cirrus regimes (homogeneous and heterogeneous). The results are for Arctic (60-90°N) during boreal winter (DJF) of 2008, 2010, 2012, and 2013 and for two different surface types: a-b) land and c-d) ocean. Markers show median values, whereas error bars show 25th and 75th percentiles.

https://doi.org/10.5194/egusphere-2025-1165
Preprint. Discussion started: 25 March 2025

studies. The reader is advised to check Mitchell and Garnier (2024) for a detailed explanation of the method for discriminating between heterogeneous and homogeneous cirrus clouds. Figure 3 shows an example of this analysis for IWC and D_e vs. height over the Arctic during the December-January-February (DJF) period. Note that each panel presents a compilation of numerous cirrus cloud samples for various heights, grid points, and days, and therefore, it is not correct to assume that it represents a single cirrus from the lowest to highest height shown. For practical purposes, the IWC and D_e apparent "profiles" from the lowest to highest height for each cirrus regime are divided into 4 clouds each having a thickness of ~ 1.3 km (Dowling and Radke, 1990; Gouveia et al., 2017), but with different cloud base and top heights (CBHs and CTHs). Each of these clouds with their respective IWC and D_e profiles are then used as input to an RTM to simulate the radiative properties for that cloud.

2.2 Radiative Transfer Model (RTM)

In this study, the calculations of various thermal or LW fluxes and solar or SW fluxes are conducted using an RTM termed library for Radiative transfer (libRadtran), which employs "uvspec" as its main core (Emde et al., 2016). For simplicity, we refer to libRadtran uvspec as RTM in the rest of this paper. The RTM solver is selected to be the one-dimensional Discrete Ordinate Radiative Transfer model (DISORT; Stamnes et al., 2000; Buras et al., 2011) with six streams. The spectral wavelength range is from 0.25 µm to 5 µm for SW and from 3.1 µm to 100 µm for LW. In addition, the REPTRAN parameterization with fine resolution is selected to account for molecular absorption (Gasteiger et al., 2014).

The RTM has the option to calculate the radiative impact of clouds based on the vertical profiles of cloud water content and effective radius (r_e) which are provided as inputs. Ice and liquid cloud properties need to be specified separately in the RTM input files. To calculate the cloud optical properties from IWC and r_e in the RTM, we specify the Baum parameterization (Baum et al., 2005) with the assumption of a general habit mixture (GHM). The GHM consists of a mixture of different ice particle shapes or habits (e.g. columns, plates, bullet rosettes, aggregates) that vary with particle size. This allows for a more realistic representation of the ice particles since cirrus clouds consist of a wide range of ice habits and sizes (Erfani and Mitchell, 2016, 2017; Lawson et al., 2019). The

https://doi.org/10.5194/egusphere-2025-1165
Preprint. Discussion started: 25 March 2025

liquid cloud parameterization of RTM follows the method of Hu and Stamnes (1993). The preparation of variables required for the atmospheric profile file is explained in Sect. 2.1.

By turning on the aerosols option in the RTM, we select the fall-winter season and the maritime haze for the atmosphere below 2 km (as boundary layer or BL) and the background for the atmosphere above 2 km (as free troposphere or FT), following the aerosol model of Shettle (1989) for the main RTM simulations. The broadband thermal emissivity (ε) varies based on the surface type. Although the ε value of snow and ice surfaces is very close to that of a blackbody (equal to unity), it is approximately 0.99 for ocean and forest, and lower for surface types such as cropland, shrubland, and deserts (Wilber et al., 1999). Nonetheless, the sensitivity of LW fluxes to ε is much smaller than that to temperature based on Stefan–Boltzmann law. Therefore, we use an ε value of unity throughout this study but conduct simulations to investigate the sensitivity to temperature.

Table 1. A summary of RTM runs conducted in this study.

Experiment	Region	Season	Surface type	Radiation	Cirrus cloud regimes	Number of simulations
Main runs using CALIPSO IWC and D_e (median, upper quartile, and lower quartile profiles)	Arctic	DJF	Land	LW	Hom, Het, Clr	25
	Arctic	DJF	Ocean	LW	Hom, Het, Clr	24
	Antarctic	JJA	Land	LW	Hom, Het, Clr	25
	Antarctic	JJA	Ocean	LW	Hom, Het, Clr	24
	NH midlatitude	DJF	Land	LW	Hom, Het, Clr	25
	NH midlatitude	DJF	Land	SW	Hom, Het, Clr	25
Sensitivity to meteorology (min and max T and q_v profiles)	Arctic	DJF	Land	LW	Hom, Het, Clr	16
Sensitivity to low clouds (with three LWC values)	Arctic	DJF	Land	LW	Hom, Het, Clr	24
Sensitivity to aerosols (two BL and two FT options)	Arctic	DJF	Land	LW	Hom, Het, Clr	32
						Total: 220

https://doi.org/10.5194/egusphere-2025-1165
Preprint. Discussion started: 25 March 2025

A summary of RTM experiments in this study is provided in Table 1. A total of 220 simulations are conducted for various regions (Arctic, Antarctic, NH midlatitude), surface type (land and ocean), and different upper-level cloud conditions (homogeneous, heterogeneous, and clear sky). Furthermore, we explore sensitivity to low liquid clouds, thermodynamic profiles, and atmospheric aerosols. In order to test the impact of low liquid cloud, we add a layer from 500 m to 1100 m (thickness of 600 m) with cloud droplet r_e of 7 μm. These values are consistent with field measurements of low clouds over the Arctic Ocean and Greenland (Järvinen et al., 2023). Three low liquid clouds are tested by varying liquid water content (LWC): 0.01, 0.03, and 0.05 g m^{-3}. To investigate the effect of thermodynamic profiles, we use the maximum and minimum T and q_v profiles in the Arctic during the winter (Fig. 2) and conduct RTM sensitivity tests. Also, four different aerosol options are explored for RTM sensitivity to aerosols: "marine haze, low volcanic", "urban haze, low volcanic", "marine haze, high volcanic", and "urban haze, high volcanic".

2.3 Cloud Radiative Effect

The change in radiative fluxes caused by cirrus clouds is quantified by the CRE following Loeb et al. (2009):

$$\mathrm{CRE}_{\mathrm{LW_z}} = \left(\mathrm{LW}\downarrow_{\mathrm{z_{cld}}} - \mathrm{LW}\uparrow_{\mathrm{z_{cld}}}\right) - \left(\mathrm{LW}\downarrow_{\mathrm{z_{clr}}} - \mathrm{LW}\uparrow_{\mathrm{z_{clr}}}\right), \quad (1)$$

where z refers to a specific height (which is either TOA or Sfc in this study], arrows indicate upward or downward fluxes, "cld" refers to the cloudy condition, and "clr" refers to the clear-sky condition. Each term is in units of W m^{-2} and all the radiative fluxes in the right-hand side of the above equation are the outputs of the RTM. As shown in Eq. (1), we consider downward fluxes as positive and vice versa throughout this study. The CRE in the Atm is calculated as:

$$\mathrm{CRE}_{\mathrm{LW_{Atm}}} = \mathrm{CRE}_{\mathrm{LW_{TOA}}} - \mathrm{CRE}_{\mathrm{LW_{Sfc}}}. \quad (2)$$

A similar set of equations is used to derive the SW CRE. In our RTM study, we use $\mathrm{CRE}_{\mathrm{LW_{Sfc}}}$ to estimate the instantaneous effect of cirrus clouds, while $\mathrm{CRE}_{\mathrm{LW_{Atm}}}$ represents the cirrus effect that could potentially influence the surface over longer timescales through adjustment and feedback processes. The net CRE is defined as:

$$\mathrm{CRE}_{\mathrm{net_z}} = \mathrm{CRE}_{\mathrm{LW_z}} + \mathrm{CRE}_{\mathrm{SW_z}}, \quad (3)$$

https://doi.org/10.5194/egusphere-2025-1165
Preprint. Discussion started: 25 March 2025

which can be calculated for the TOA, Sfc, or Atm. In this study, we define CCT as the transition from homogeneous to heterogeneous cirrus and calculate its efficacy, ΔCRE, as the difference in CRE between homogeneous and heterogeneous:

$$\Delta\mathrm{CRE} = \langle \mathrm{CRE}_{\mathrm{het}} - \mathrm{CRE}_{\mathrm{hom}} \rangle, \quad (4)$$

where angle brackets show the average for the four cirrus clouds at 4 different altitudes, as explained in Sect. 2.1. Note that ΔCRE is based on the ideal assumptions that cirrus cloud overcast condition exists. Therefore, correction factors are required for more realistic impact:

$$\Delta\mathrm{CRE}_t = \Delta\mathrm{CRE} \times \mathrm{CF}_{\mathrm{cirrus}} \times \mathrm{F}_{\mathrm{hom}}, \quad (5)$$

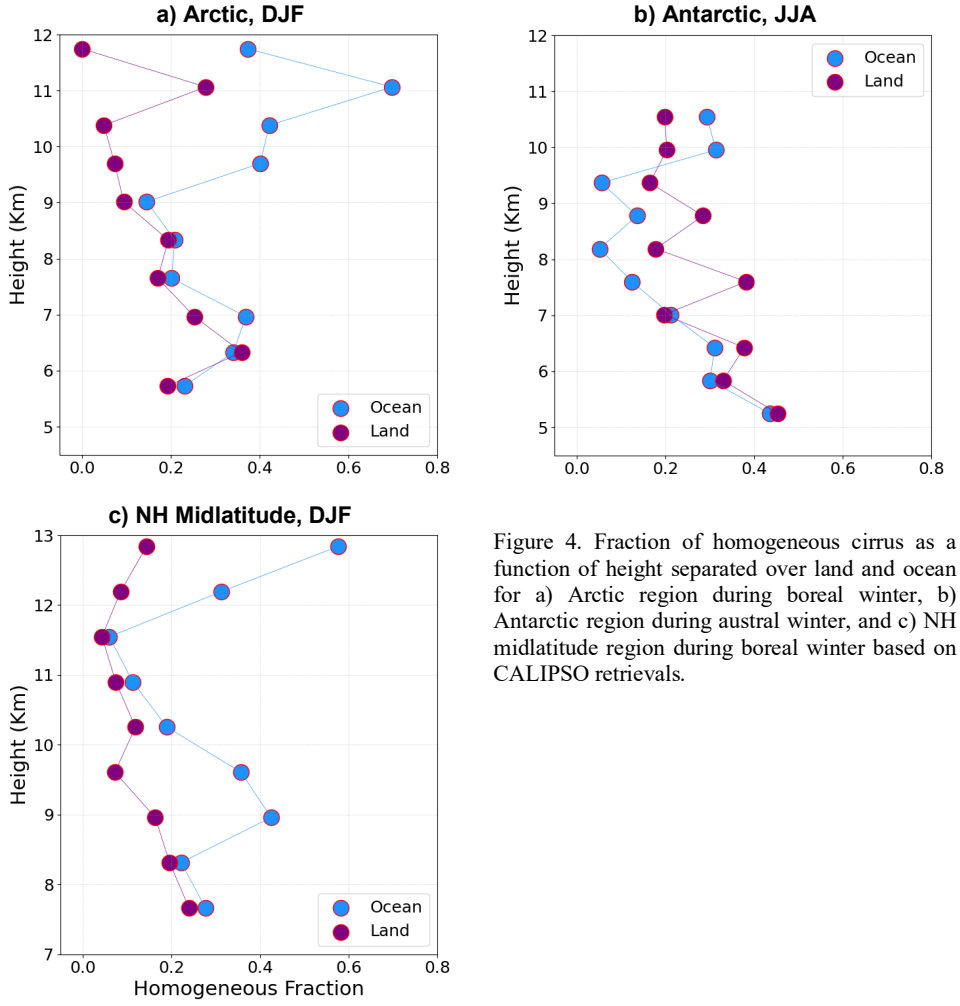

Figure 4. Fraction of homogeneous cirrus as a function of height separated over land and ocean for a) Arctic region during boreal winter, b) Antarctic region during austral winter, and c) NH midlatitude region during boreal winter based on CALIPSO retrievals.

https://doi.org/10.5194/egusphere-2025-1165
Preprint. Discussion started: 25 March 2025

where CF_{cirrus} is cirrus cloud fraction and F_{hom} is fraction of homogeneous cirrus clouds. The CALIPSO cirrus cloud analysis of Mitchell and Garnier (2024) does not explicitly provide values of CF_{cirrus}. Therefore, we use a typical value of 35% for extratropical regions (Gasparini et al., 2023). This estimate may be conservative for the polar regions during winter when ice cloud coverage appears greater than in other seasons (Hong et al., 2016; Mitchell et al., 2018; Sassen et al., 2009). The retrievals provide vertical profiles of the homogeneous fraction (defined as the number of homogeneous cirrus pixels divided by the total number of cirrus pixels) for different regions and seasons as shown in Fig. 4. Strong variability is seen in homogeneous fraction with height, region (Arctic, Antarctic, and midlatitude), and surface type (land and ocean) and this makes it important to conduct a different RTM simulation for each of those geographical conditions. We use the IWC-weighted average of the homogeneous fraction to calculate F_{hom}. In this study, Sfc ΔCRE_t is used to estimate the instantaneous efficacy of CCT, while Atm ΔCRE_t represents the potential CCT effect—that is, the extent to which changes in atmospheric heating due to CCT could ultimately influence the surface through climatic feedback processes.

3 Main RTM simulations

3.1 Arctic region

The RTM simulations are conducted using mean thermodynamic profiles from MERRA2 for the Arctic during the boreal winter (Fig. 2) and ice cloud properties using the median, 25th and 75th percentile IWC and D_e from CALIPSO satellite retrievals, as shown in Fig. 3. A general pattern of cirrus cloud properties is seen in Fig. 3 (e.g., a decrease in both IWC and D_e with height, which is characteristic of cirrus clouds). The difference in IWC between homogeneous and heterogeneous cirrus is distinct, as homogeneous cirrus in our CALIPSO retrievals have much larger IWC than heterogeneous cirrus at the same altitude, in agreement with previous studies (Krämer et al., 2016, 2020). However, D_e values are similar in both cirrus regimes, which results from the criteria applied to define heterogeneous and homogeneous cirrus clouds in Mitchell and Garnier (2024). That is, when D_e is plotted against either the SW α_{ext} or IWC as shown in Fig. S1, there is generally a D_e maximum that divides the two cirrus regimes for a given T. The maximum in the number of

https://doi.org/10.5194/egusphere-2025-1165
Preprint. Discussion started: 25 March 2025

CALIPSO cirrus cloud samples when related to α_{ext} or IWC tends to coincide with this D_e maximum, resulting in similar mean D_e values for each cirrus regime. But as α_{ext} or IWC increases beyond this D_e maximum, D_e decreases, which is consistent with conventional knowledge that an increase in homogeneous ice nucleation activity will act to increase N_i and decrease particle sizes due to water vapor competition effects.

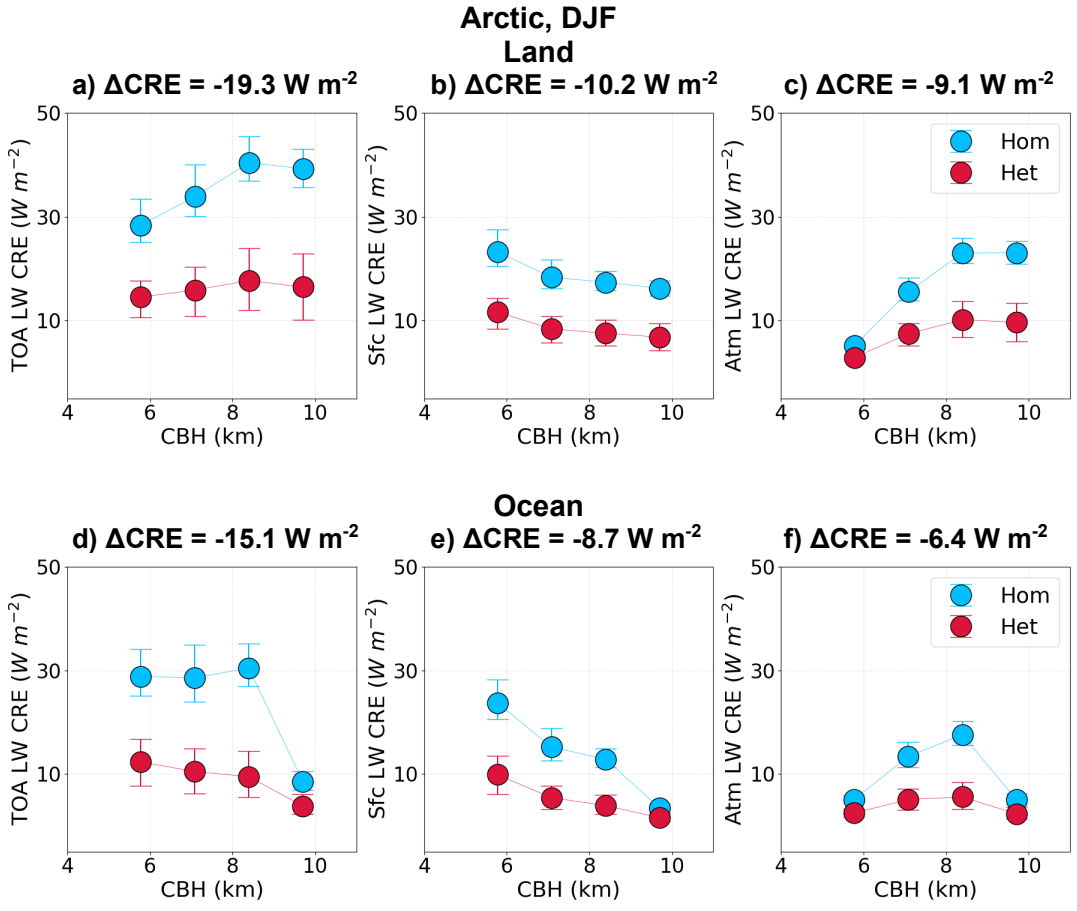

Figure 5. Results of RTM simulations showing LW CRE as a function of CBH over the Arctic during the boreal winter for 4 cirrus clouds separated based on surface types (land and ocean) and cirrus regimes (homogeneous and heterogeneous). The CRE is calculated at the TOA, at the surface, and within the column of atmosphere. The ΔCRE at the top of each panel represent the transition from homogeneous to heterogeneous cirrus based on Eq. (5). A total of 48 RTM simulations are shown in this figure with markers and error bars referring to simulations based on CALIPSO profiles in Fig. 4.

https://doi.org/10.5194/egusphere-2025-1165
Preprint. Discussion started: 25 March 2025

Due to different cloud properties over land and ocean, different RTM simulations are conducted for land and ocean. Figure 5 shows TOA, Sfc, and Atm LW CRE calculated from RTM simulations using Eqs. (1) and (2). Note that no RTM simulation is conducted for SW range because of the absence of solar radiation in this region during the winter. As such, these results serve as net CRE (Eq. 3). LW CRE in Fig. 5 varies with CBH, highlighting the effects of cirrus cloud altitude as well as microphysical properties. The LW CRE at the surface generally decreases with CBH because colder clouds at higher altitudes emit less LW compared to warmer clouds at lower altitudes, based on the Stefan–Boltzmann law. In addition, cirrus clouds at higher altitudes often have lower IWC (Fig. 3), and this makes them optically thinner. In contrast, smaller D_e in cirrus at higher altitudes could lead to stronger LW CRE (Fu and Liou, 1993). At the TOA, LW CRE depends on the difference between the cloud's LW emission and the emission from the Earth's surface (Corti and Peter, 2009), and such difference is larger for cirrus at higher altitudes.

Also seen in Fig. 5 is significantly larger LW CRE at the TOA, at the Sfc, and within the Atm for homogeneous cirrus than that for heterogeneous cirrus of the same altitude. This is mainly due to higher IWC values for homogeneous cirrus (Fig. 3), which leads to optically thicker cirrus (Krämer et al., 2016, 2020). When both cirrus regimes have comparable IWC, as seen for the highest altitude over the ocean, their LW CRE is comparable. This highlights the critical role of IWC in determining the radiative impact of cirrus clouds.

Over land, the CCT efficacy, defined as the transition from homogeneous to heterogeneous cirrus and quantified by ΔCRE in Eq. (4), results in a TOA cooling effect of -19.3 W m^{-2} (the mean value of the four clouds considered), with a corresponding Sfc cooling of -10.2 W m^{-2} and atmospheric column cooling of -9.1 W m^{-2} (Figs. 5a-c). Considering that the typical cirrus cloud cover over the Arctic is 35% and that the IWC-weighted average of the homogeneous fraction is 0.21 (Fig. 4a), Eq. 5 gives the total cooling effect ΔCRE_t at the TOA, Sfc, and Atm as ~ -1.4, -0.7, and -0.7 W m^{-2}, respectively (Table 2). Of particular importance for CCT is the cooling at the surface but note that the RTM provides instantaneous values. For the atmospheric column, the RTM calculates a cooling effect that is similar to the surface cooling. This might have implications for long-term feedback processes and possibly impact AA, as the atmospheric column cooling could lead to lower geopotential thickness over the Arctic, which in turn might affect meridional T gradients,

https://doi.org/10.5194/egusphere-2025-1165
Preprint. Discussion started: 25 March 2025

thermal winds, and the extratropical jet stream (Cohen et al., 2020). However, a careful GCM study is required to test this hypothesis.

The overall pattern of cooling over the ocean is consistent with that over land, but the cooling effect over the ocean is slightly weaker, with a TOA ΔCRE of -15.1, a Sfc ΔCRE of -8.7 W m^{-2} and an Atm ΔCRE of -6.4 W m^{-2} (Figs. 5d-f). With a typical cirrus cloud cover value of 35% and IWC-weighted mean homogeneous fraction of 0.29 (Fig. 4a) over the ocean, TOA, Sfc, and Atm $\Delta\mathrm{CRE}_t$ are approximately -1.5, -0.9, and -0.6 W m^{-2}, respectively (Table 2). These values are higher than $\Delta\mathrm{CRE}_t$ over land because of the higher homogeneous fraction over the ocean. Note that in Mitchell and Garnier (2024), regions consisting of sea ice are considered as land. As shown in Fig. S2a, the higher sea ice fraction in winter along with the pure land fraction constitutes a much larger area than water surfaces. As such, $\Delta\mathrm{CRE}_t$ over the ocean makes a smaller impact. Nevertheless, we conduct analysis for both land and ocean for a more comprehensive analysis.

3.2 Antarctic region

The RTM simulations for the Antarctic are conducted similarly to those for the Arctic, using mean thermodynamic profiles from MERRA2 (not shown) and median, 25th and 75th percentile IWC and D_e profiles from CALIPSO satellite retrievals (Fig. 6) during the austral winter for this region. While the general patterns of IWC and D_e profiles for homogeneous and heterogeneous cirrus are similar to those in the Arctic, the specific values and details differ between the two regions. Simulations are performed for both land and ocean, and the LW CRE (equivalent to net CRE due to the absence of SW radiation during austral winter) is calculated at the TOA, Sfc, and Atm, as shown in Fig. 7.

Table 2. Quantifying the transition from homogeneous to heterogeneous cirrus (for overcast skies) using the change in their cloud radiative effect (ΔCRE) and its total value that assumes 35% cloud coverage ($\Delta\mathrm{CRE}_t$) at various levels based on Eq. (5) for different regions, seasons, and surface types.

Region	Season	Surface type	F_{hom}	ΔCRE (W m^{-2})			$\Delta\mathrm{CRE}_t$ (W m^{-2})		
				TOA	Sfc	Atm	TOA	Sfc	Atm
Arctic	DJF	Land	0.21	-19.3	-10.2	-9.1	-1.4	-0.7	-0.7
		Ocean	0.29	-15.1	-8.7	-6.4	-1.5	-0.9	-0.6
Antarctic	JJA	Land	0.3	-15.4	-9.2	-6.2	-1.6	-1.0	-0.6
		Ocean	0.24	-13.7	-9.3	-4.3	-1.2	-0.8	-0.4
NH midlat	DJF	Land	0.15	-22.9	+0.2	-23.1	-1.2	0.0	-1.2

https://doi.org/10.5194/egusphere-2025-1165
Preprint. Discussion started: 25 March 2025

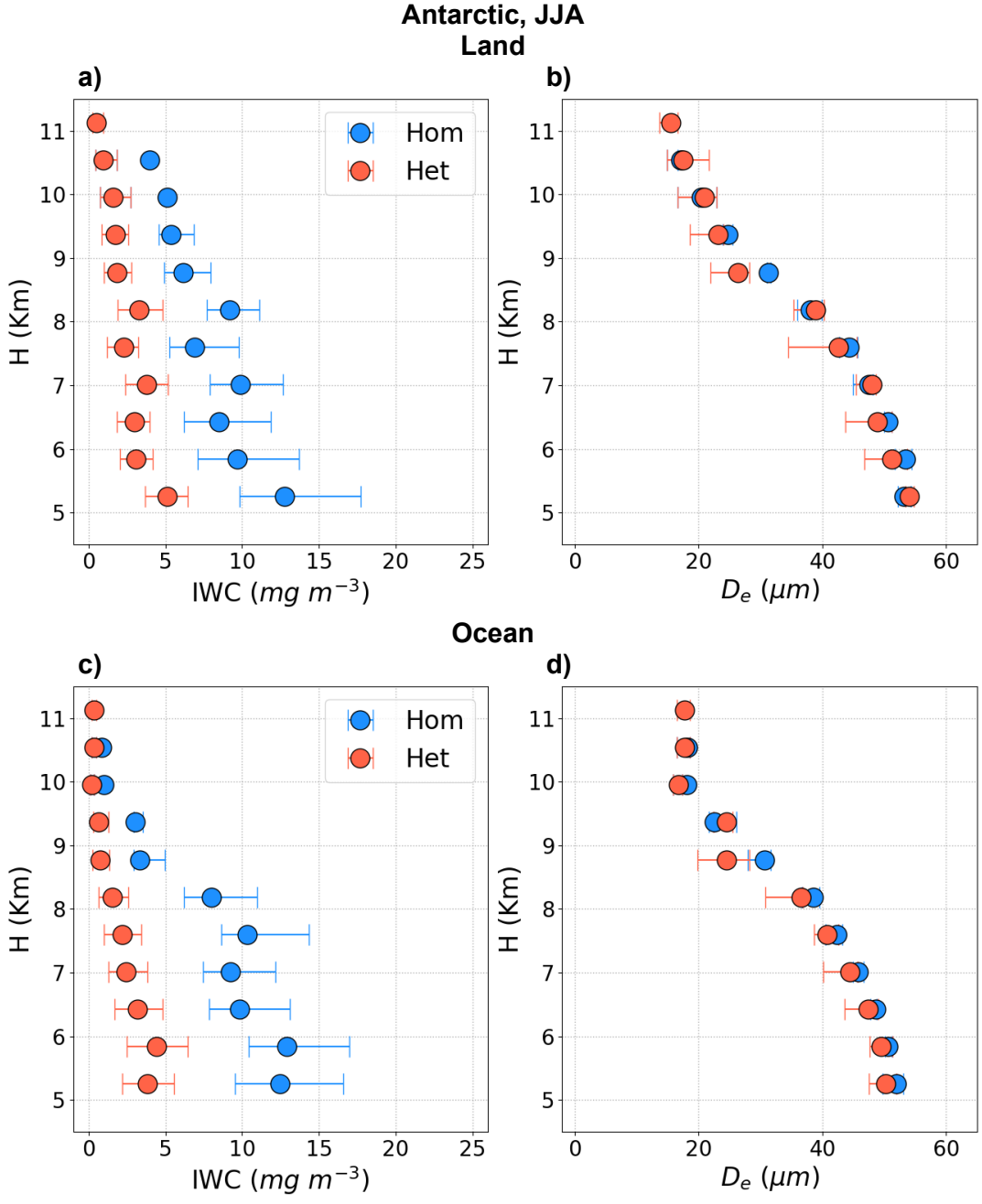

Figure 6. As in Fig. 3, but the results are for Antarctic (90-60°S) during austral winter (JJA).

https://doi.org/10.5194/egusphere-2025-1165
Preprint. Discussion started: 25 March 2025

The TOA CRE over Antarctic land is weaker than that over the Arctic for cirrus clouds at the same altitude, particularly for homogeneous cirrus at the two lowest altitudes. This is likely due to lower IWC in the lowest altitudes over the Antarctic compared to the Arctic (Figs. 3 and 6). As a result, the transition from homogeneous to heterogeneous cirrus, quantified by ΔCRE, leads to a TOA cooling of -15.4 W m^{-2}, which is roughly 20% weaker than the ΔCRE over Arctic land. The Sfc and Atm ΔCRE values are -9.2 W m^{-2} (~ 10% weaker than that over the Arctic land), and -6.2 W m^{-2} (~ 40% weaker than that over the Arctic land), respectively. Despite the lower IWC for homogeneous cirrus over the Antarctic, the homogeneous fraction is significantly higher (IWC-weighted average is 0.30), resulting in stronger total cooling over the Antarctic than over the Arctic; the total cooling effects (ΔCRE_t) at the TOA, Sfc, and Atm are approximately -1.6, -1.0, and -0.6 W m^{-2}, respectively (Table 2).

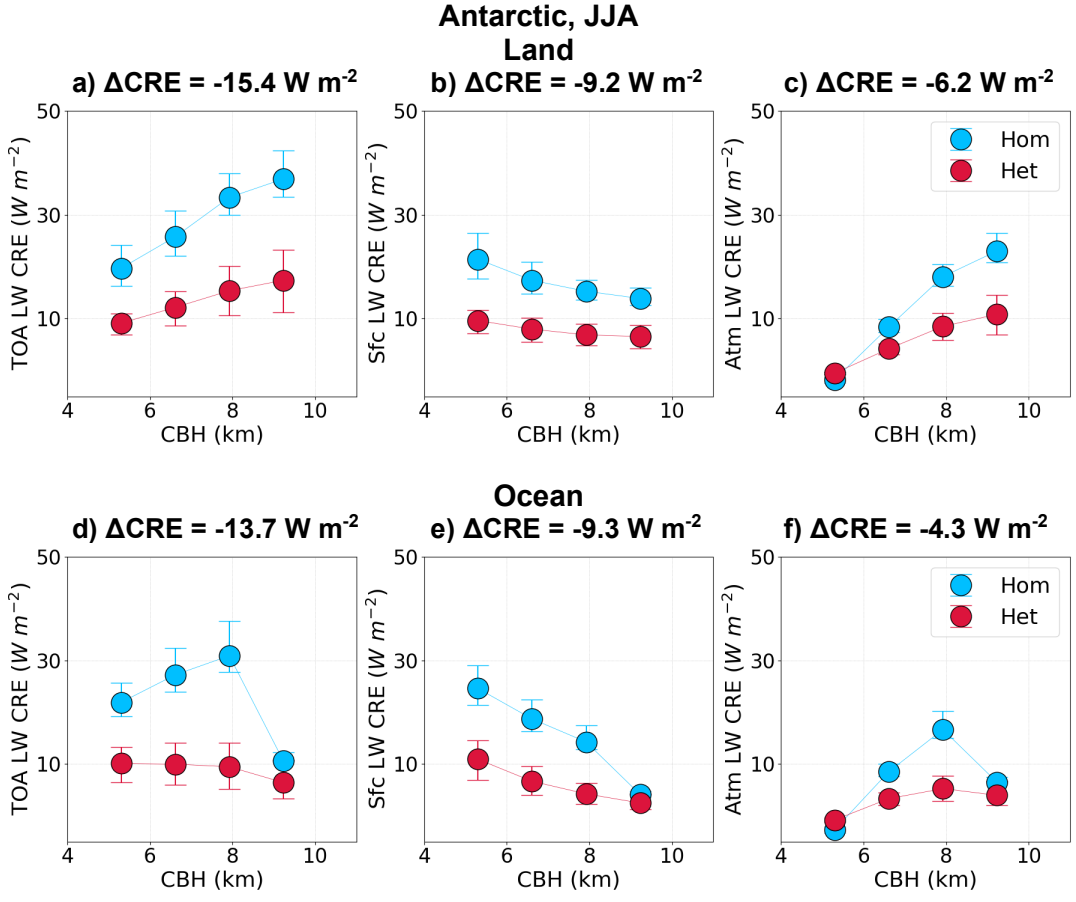

Figure 7. As in Fig. 5, but the results are RTM simulations for Antarctic during austral winter.

https://doi.org/10.5194/egusphere-2025-1165
Preprint. Discussion started: 25 March 2025

Over the ocean, the TOA cooling effect (ΔCRE) is weaker compared to all previous results in this study. The TOA, Sfc, and Atm ΔCRE values are estimated to be -13.7, -9.3, and -4.3 W m^{-2}, respectively. With an IWC-weighted average homogeneous fraction of 0.24, ΔCRE_t at the TOA, Sfc, and Atm are approximately -1.2, -0.8, and -0.4 W m^{-2}, respectively (Table 2). These values are weaker than those for Antarctic land and Arctic land and ocean. However, for the Antarctic, the CCT cooling effect over the ocean is much smaller than that over land, given that the surface water fraction is much smaller than the fraction of sea ice and the Antarctic land mass during austral winter (Fig. S2b).

To the best of our knowledge, no previous study has used an RTM to estimate the cooling efficacy of CCT. Although the instantaneous surface cooling in our study for both polar regions and over land and ocean (Sfc ΔCRE_t: -0.7 to -1.0 W m^{-2}) and the TOA cooling (TOA ΔCRE_t: -1.2 to -1.6 W m^{-2}) are much weaker than the potential cooling of -2.8 W m^{-2} suggested by Mitchell and Finnegan (2009), they fall within the range of maximum CCT cooling from previous GCM studies, from -0.25 W m^{-2} (Gasparini and Lohmann, 2016) to -2 W m^{-2} (Storelvmo et al., 2013; Storelvmo and Herger, 2014). We acknowledge that this is not a direct comparison, as GCMs calculate global CREs while accounting for feedback processes. However, we note that CCT in the polar regions during winter could be as effective as CCT applied globally throughout the year, as the significant LW trapping by cirrus clouds outside the polar regions is counteracted by SW scattering (Storelvmo et al., 2014).

3.3 North hemispheric mid-latitude region

Mid-latitude regions (30°N to 60°N and -60°S to -30°S latitude bands) comprise approximately 37% of the Earth's surface, which is about three times the area of the high latitudes. This makes it important to evaluate the potential efficacy of CCT in these regions. During winter, the SW impact of cirrus clouds is minimized due to shorter days and higher solar zenith angles (SZA). The SZA, which quantifies the position of the Sun (ranging from 0° at the equator at midday during an equinox to 90° at sunrise and sunset), has a daytime average of 73° at 45°N latitude during the winter solstice (Hartmann, 2016). In addition to LW RTM simulations, we conduct SW simulations for a daytime average winter solstice mid-latitude scenario: 45°N latitude, a surface albedo of 0.3, and an SZA of 73°. The RTM is forced with mean thermodynamic profiles

https://doi.org/10.5194/egusphere-2025-1165
Preprint. Discussion started: 25 March 2025

from MERRA2 (not shown) and median, 25th, and 75th percentile IWC and D_e profiles from CALIPSO satellite retrievals (Fig. S3) during the boreal winter for NH mid-latitude land.

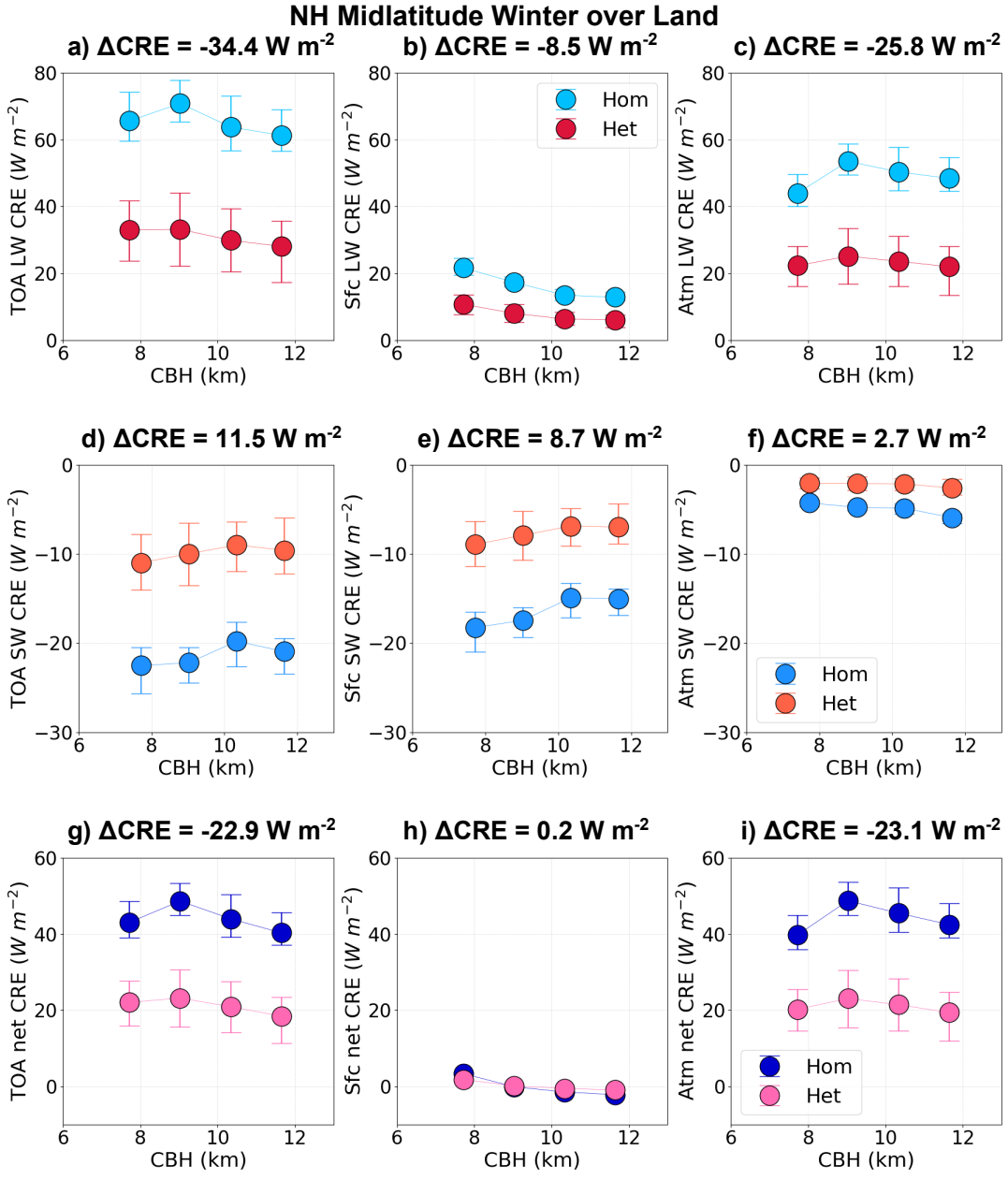

Figure 8. As in Fig. 5, but the results are RTM simulations for LW, SW, and net CRE over NH midlatitude land with a total of 50 RTM simulations.

https://doi.org/10.5194/egusphere-2025-1165
Preprint. Discussion started: 25 March 2025

The results of the RTM simulations for various CREs are shown in Fig. 8. The LW CRE at the TOA over mid-latitudes is significantly larger than that over polar regions for cirrus clouds of the same regime (homogeneous or heterogeneous) and at the same altitude. This is likely due to higher IWC within cirrus clouds (Fig. S3) and a warmer temperature profile for midlatitudes compared to polar regions. Cirrus clouds with higher IWC trap more LW radiation, resulting in stronger LW CRE (Fu and Liou, 1993). Furthermore, the warmer temperature profile and in particular warmer surface in mid-latitudes emit more LW radiation toward the upper troposphere, which is absorbed and re-emitted at colder temperatures by cirrus clouds. This causes a stronger difference between LW emitted by cirrus cloud and Earth's surface and enhances the TOA LW CRE (Corti and Peter, 2009).

The SW CRE (Figs. 8d–f) is calculated to provide daily-mean values. To account for the diurnal cycle of SW radiation, the SW CRE from Eqs. (1) and (2) is multiplied by a factor of 0.37, representing the ratio of daytime hours (8.8 hours) to 24 hours at 45°N latitude during the winter solstice. This post-simulation factor, combined with the daytime-average SZA used in the RTM simulations, averages the SW CRE at 45°N over a full 24-hour period, consistent with the LW CRE calculations. All SW CRE values are negative, indicating the cooling effect of cirrus clouds at different altitudes and with various microphysical properties due to the absorption and scattering of solar radiation. Homogeneous cirrus clouds exhibit significantly stronger SW cooling effects than heterogeneous cirrus clouds at the TOA and Sfc, as they contain higher IWC, which corresponds to greater scattering and absorption by ice particles (Fu and Liou, 1993). The change in SW CRE with cloud altitude depends on changes in α_{ext}, where $\alpha_{ext} = 3\ \mathrm{IWC}/(\rho_i\ D_e)$, and ρ_i is bulk density of ice. As cloud altitude increases, both IWC and D_e decrease, resulting in a relatively slow decrease in α_{ext} with increasing altitude (Fu and Liou, 1993; Stephens et al., 1990).

The transition from homogeneous to heterogeneous cirrus results in a surface LW cooling (ΔCRE) of -8.5 W m^{-2}, which is largely offset by SW warming (ΔCRE = 8.7 W m^{-2}), leading to a relatively small net surface ΔCRE of -0.2 W m^{-2} (Fig. 8h). At the TOA, the strong difference in LW CRE between the two regimes results in significant LW cooling (ΔCRE = -34.4 W m^{-2}), which is partially offset by SW warming (ΔCRE = 11.5 W m^{-2}), yielding a net TOA cooling of -22.9 W m^{-2} (Fig. 8g). Within the atmospheric column, a significant net cooling of -23.1 W m^{-2} occurs (Fig. 8i). Considering an IWC-weighted average homogeneous fraction of 0.15 (Fig. 4c) and a cirrus

https://doi.org/10.5194/egusphere-2025-1165
Preprint. Discussion started: 25 March 2025

525 cloud cover of 35%, the total net cooling effects (ΔCRE_t) at the TOA, Sfc, and Atm are approximately -1.2, 0.0, and -1.2 W m^{-2}, respectively (Table 2). These results demonstrate that while the instantaneous cooling efficacy of CCT (Sfc net ΔCRE) in mid-latitudes during winter is negligible, CCT could still be effective if its impact on the atmospheric column (Atm net ΔCRE_t) can reach the surface through feedback processes.

530

4 Sensitivity tests

4.1 Sensitivity to thermodynamic profiles

The impact of temperature and humidity on cirrus LW CRE is evaluated using minimum and maximum air T and q_v profiles (referred to as T_{min} and T_{max} for brevity) from MERRA2 data for
535 Arctic land during the winter (Fig. 9). TOA LW CRE significantly increases with an increase in T and q_v. In particular, Earth's surface plays an important role because it typically acts as a blackbody (its ε is very close to unity), and even a rather small surface warming can significantly enhance LW radiation emitted from the surface, as described by Stefan–Boltzmann law. With unchanged cirrus temperature and LW emission, the enhanced upward LW radiation from the Earth's surface
540 creates a stronger LW contrast, resulting in a stronger TOA LW CRE (Corti and Peter, 2009).

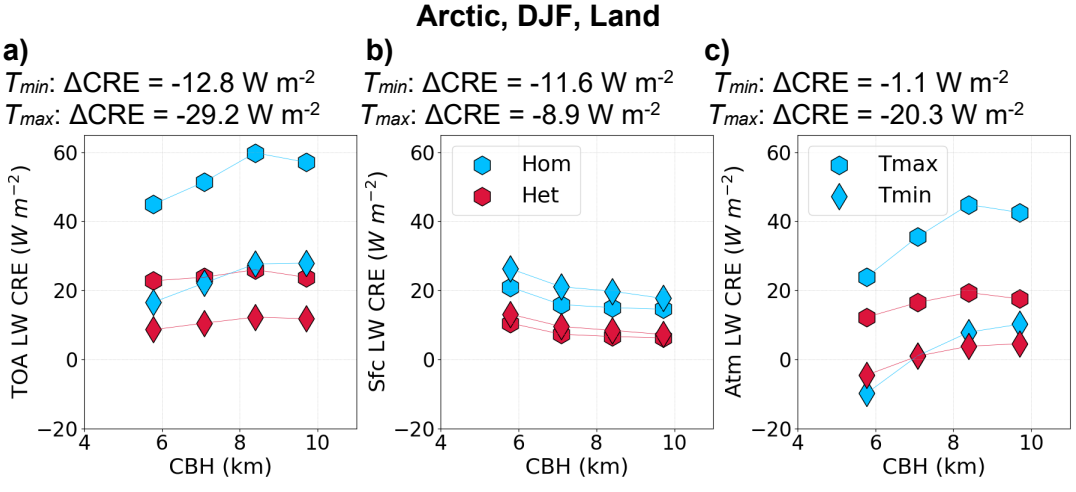

545

Figure 9. Sensitivity of RTM-simulated cirrus CRE to different thermodynamic profiles from MERRA2 minimum and maximum temperature and water mixing ratio (abbreviated as T_{min} and T_{max}), as shown in Fig. 2.

https://doi.org/10.5194/egusphere-2025-1165
Preprint. Discussion started: 25 March 2025

At the surface, however, LW CRE is weakly sensitive to thermodynamic profiles (Fig. 9b). Profiles with lower T and q_v lead to slightly higher cirrus LW CRE at the surface, particularly for homogeneous cirrus. The surface LW CRE depends primarily on the downward LW radiation from cirrus clouds, rather than surface temperature (Eq. 1). Therefore, the lower surface LW CRE in maximum profiles compared to minimum profiles is due to higher water vapor in the atmosphere, which absorbs part of the downward LW radiation from cirrus clouds before it reaches the surface. This is consistent with the findings of Dupont and Haeffelin (2008).

Figure 9a shows that the transition from homogeneous to heterogeneous cirrus (ΔCRE) intensifies significantly with warmer and more humid thermodynamic profiles, particularly with higher surface temperatures. The ΔCRE for minimum and maximum profiles is -12.8 W m^{-2} and -29.2 W m^{-2}, respectively. At the surface (Fig. 9b), the ΔCRE for minimum and maximum profiles is -11.6 W m^{-2} and -8.9 W m^{-2}, respectively, indicating minimal sensitivity to thermodynamic profiles. This consistency suggests that the instantaneous CCT efficacy is robust across different thermodynamic conditions. However, the atmospheric ΔCRE (Fig. 9c) shows greater variability, ranging from -1.1 W m^{-2} for the minimum thermodynamic profile to -20.3 W m^{-2} for the maximum profile, highlighting the sensitivity of potential CCT efficacy to thermodynamic profiles.

4.2 Sensitivity to Arctic low clouds

Low clouds are frequent over the Arctic region and they have a significant impact on the radiation balance (Philipp et al., 2020). These clouds are controlled by many factors including atmospheric circulation and sea ice extent and in return, they impact the sea ice via an ice-albedo feedback (Huang et al., 2021). During the winter, low clouds trap outgoing longwave radiation and warm the surface, but during the summer, this effect is canceled by cooling from reflecting solar radiation (Maillard et al., 2021). Arctic low cloud cover varies by season and this variability is more distinct for higher latitudes of the Arctic (north of latitude 70) where low cloud cover changes from over 50% in summer to lower than 20% in winter (Eastman and Warren, 2010). Arctic low clouds tend to have higher cloud water path (CWP) over the open ocean and lower CWP over ice-covered areas (Yu et al., 2019) due to higher moisture availability over the ocean than ice (Monroe et al., 2021). The spatial distribution of arctic low clouds shows that over land their cover is typically around 35% in summer and around 15% in winter. Over the ocean, their cover is around 55% in

https://doi.org/10.5194/egusphere-2025-1165
Preprint. Discussion started: 25 March 2025

summer, but drops below 30% on the Pacific side of the Arctic Ocean, meanwhile remains as high as 50% on the Atlantic side of the Arctic Ocean in winter (Huang et al., 2021).

Our RTM simulations explore the impact of low liquid clouds on cirrus CRE by introducing a low liquid cloud layer, as described in Sect. 2. Three low liquid clouds are tested by varying LWC (e.g., 0.01, 0.03, and 0.05 g m^{-3}). To calculate cirrus CRE using Eq. (1), we consider the difference between an RTM run with both cirrus and low liquid cloud versus an RTM run with only low liquid cloud.

The results (Fig. 10) show that TOA LW CRE for cirrus clouds is not sensitive to the low liquid clouds. Over the Arctic, such clouds are close to the surface, and their temperature is very similar to that of the Earth's surface (due to inversion, mean profile of *T* in Fig. 2a varies slowly below 2 km). As a result, the LW radiation emitted by low liquid clouds is close to that emitted by Earth's surface. Moreover, we only vary the LWC of low clouds, not their elevation, so their temperature remains constant. Consequently, the difference between cirrus LW radiation and the upward LW radiation from the underlying clouds and Earth's surface does not change significantly across the three sensitivity tests in this section.

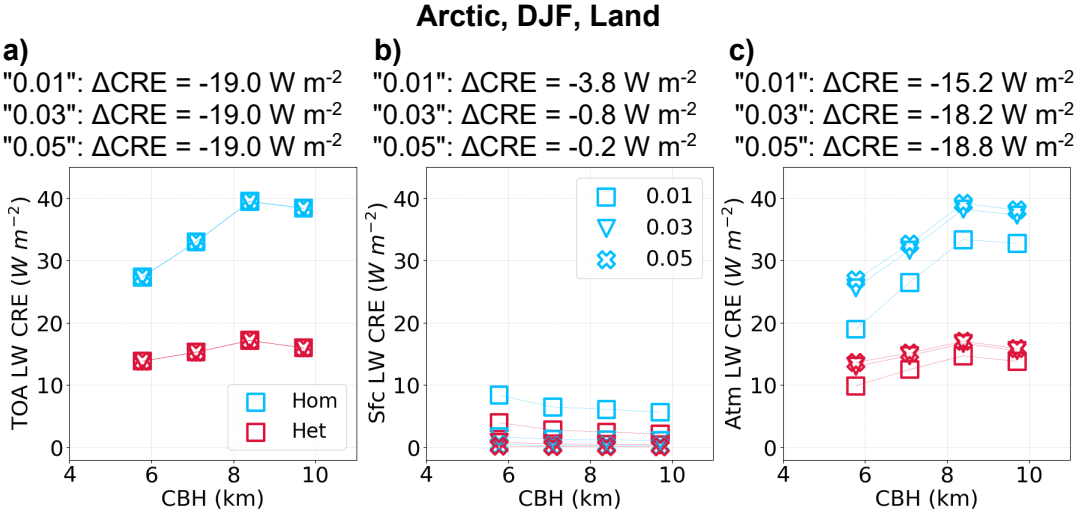

Figure 10. Sensitivity of RTM-simulated cirrus CRE to three different low liquid clouds with varying liquid water content (LWC) values of 0.01, 0.03, and 0.05 g m^{-3}.

https://doi.org/10.5194/egusphere-2025-1165
Preprint. Discussion started: 25 March 2025

At the surface, however, cirrus LW CRE decreases rapidly as low cloud LWC increases. Note that the largest LWC selected here (0.05 g m^{-3}) is at the lower end of typical LWC values observed in the Arctic (Achtert et al., 2020). Our results demonstrate that low liquid clouds ~ 600 m thick with a LWC greater than 0.05 g m^{-3} act more like a "black body", absorbing/emitting almost all the downward LW radiation emitted by cirrus clouds.

The presence of low clouds has little effect on the transition from homogeneous to heterogeneous cirrus at the TOA, with ΔCRE remaining at −19.0 W m^{-2}. However, it considerably reduces ΔCRE at the surface, from −3.8 W m^{-2} (for LWC = 0.01 g m^{-3}) to −0.2 W m^{-2} (for LWC = 0.05 g m^{-3}). As a result, the atmospheric ΔCRE remains between −15.2 W m^{-2} and −18.8 W m^{-2}. These results imply that while the instantaneous efficacy of CCT is negligible in the presence of low liquid clouds, its potential efficacy could still influence the surface through feedback processes over longer timescales.

4.3 Sensitivity to Arctic aerosols

In the past, the Arctic atmosphere was considered pristine, but over the past decades, it has been revealed that Arctic aerosols play an important role through aerosol-radiation interactions (Thorsen and Fu, 2015) and aerosol-cloud interactions (Creamean et al., 2021; Zamora et al., 2016). Both observations (Dagsson-Waldhauserova et al., 2019) and numerical simulations (Breider et al., 2014) showed that Arctic aerosol concentrations vary with season with the main peak in late winter and spring, and another peak in fall. The major peak is known as the Arctic haze, a phenomenon mainly caused by the transport of industrial anthropogenic aerosols from Europe and Asia that remain in the Arctic atmosphere due to a stable atmosphere and a lack of precipitation (Schmale et al., 2022). With the reduction of anthropogenic aerosols in summer, natural aerosols, including sea spray and organic compounds, dominate (Moschos et al., 2022). Another important aerosol type in the Arctic is dust with its maximum in late winter and early spring due to the long-range transport from Asia and Africa and its minimum in summer and fall predominantly because of local sources (Groot Zwaaftink et al., 2016; Xie et al., 2022).

Our RTM simulations evaluate the sensitivity of cirrus CRE to different aerosol scenarios, as explained in Sect. 2. The results (Fig. S4) show that aerosol type and concentration have a

https://doi.org/10.5194/egusphere-2025-1165
Preprint. Discussion started: 25 March 2025

relatively small impact on cirrus LW CRE. This finding is consistent with previous studies, which have demonstrated that while aerosols absorb SW radiation, they are weak absorbers of LW radiation (Bergstrom et al., 2007; Samset et al., 2018). As a result, the cooling effect of transitioning from homogeneous to heterogeneous cirrus is not sensitive to the choice of aerosol scenarios, with TOA ΔCRE ranging from -19.3 to -19.8 W m^{-2}, Sfc ΔCRE from -10.2 to -10.4 W m^{-2}, and Atm ΔCRE from -9.1 to -9.4 W m^{-2}. It is important to note that the modeling design here only accounts for the aerosol direct effect, as the RTM cannot simulate aerosol indirect effects. However, it would be possible to study such effect if cloud profiles are carefully explored and grouped based on aerosol loading.

5 Suggestions for improving cirrus cloud modeling

In previous sections, we implemented satellite retrievals in an RTM to estimate the instantaneous cirrus CRE. RTMs have fewer degrees of freedom than GCMs, and this makes them more convenient for interpreting changes in cirrus radiative impacts. However, GCMs are the ultimate tool for determining the global cirrus CRE since they account for climate feedback processes which are expected to enhance the CRE predicted by an RTM. That is, the direct CCT polar cooling predicted by an RTM may promote coverage by snow and sea ice (Storelvmo et al., 2014), enhancing planetary albedo and thus cooling. Despite their advantages, GCMs face several challenges in accurately representing cirrus clouds, particularly in the distinction between the two cirrus regimes and the treatment of "*pre-existing ice*". Below, we briefly discuss these issues and propose improvements based on recent research.

5.1 Improved representation of homogeneous and heterogeneous regimes

Not all processes related to formation and dissipation of cirrus clouds can be represented in a GCM, and various GCMs employ different ice parameterizations. Most, if not all, GCMs employ ice parameterizations that are based on limited observations and therefore, uncertainties could arise when generalizing those formulations (Eidhammer et al., 2017; Gettelman and Morrison, 2015). In particular, many field campaigns do not sample homogeneous cirrus clouds sufficiently. In Figure 11, we compare D_e values from Mitchell and Garnier (2024) CALIPSO retrievals with

https://doi.org/10.5194/egusphere-2025-1165
Preprint. Discussion started: 25 March 2025

the D_e scheme from Sun and Rikus (1999) and Sun (2001), hereafter referred to as the SR99-S01 scheme. The SR99-S01 scheme is based on field campaign data and estimates D_e from IWC and T, using the following simple relationship: $D_e = a + b(T + 190)$, where $a = 45.8966(\mathrm{IWC})^{\mathbf{0.2214}}$, and $b = 0.7957(\mathrm{IWC})^{0.2535}$. SR99-S01 scheme is broadly consistent with the CALIPSO retrievals, but there are notable differences. Specifically, the SR99-S01 scheme exhibits a weaker temperature dependence and larger D_e values at low and very high IWCs compared to our retrievals. Importantly, the SR99-S01 scheme does not capture the behavior of homogeneous cirrus, where D_e decreases with increasing IWC at higher IWCs. This is likely because homogeneous nucleation events are underrepresented in field campaigns, which form the basis of the SR99-S01 scheme. The CALIPSO retrievals, however, clearly show this behavior. This highlights the value of satellite observations in complementing field campaign data and improving cirrus cloud modeling.

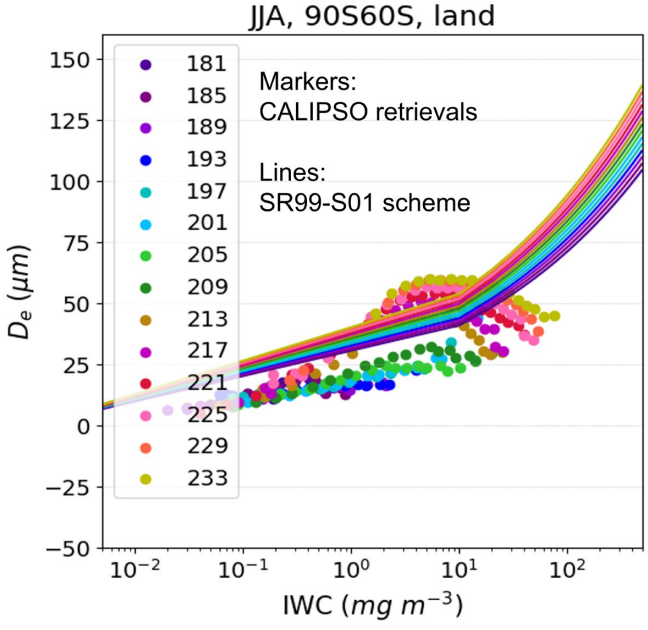

Figure 11. The results of CALIPSO retrievals (markers) for Antarctic land during the austral winter and SR99-S01 scheme (lines) showing D_e vs. IWC. See the main text for SR99-S01 equations relating D_e to IWC and T. Each marker is not a single data point, but the mean value of all data points within a 4-K temperature bin and a 0.1 log of extinction coefficient bin. Each color shows a different temperature bin with their middle point value in the legend in units of K.

https://doi.org/10.5194/egusphere-2025-1165
Preprint. Discussion started: 25 March 2025

Current GCMs might underestimate the contribution of homogeneous nucleation, particularly in the Arctic and Antarctic, where INP concentrations are low. This can lead to an underestimation of the radiative effects of cirrus clouds and the potential cooling efficacy of CCT. To address this, GCMs could use satellite retrievals of N_i, D_e, and IWC when developing parameterizations that represent the two cirrus regimes.

5.2 Treatment of pre-existing ice

A critical factor in modeling cirrus clouds is the treatment of pre-existing ice, which refers to ice particles already present before the formation of new ice particles. This treatment enhances the contribution of heterogeneous nucleation (i.e., the larger the pre-existing IWC is, the less likely homogeneous cirrus will form). Therefore, including pre-existing ice in GCMs significantly reduces N_i, as shown in simulations comparing models with and without pre-existing ice (Shi et al., 2015). Moreover, the current treatment of pre-existing ice in GCMs overestimates the pre-existing ice effect (Mitchell and Erfani, 2025; Mitchell and Garnier, 2024). That is, remote sensing observations show that RH_i is highest near cloud tops (Dekoutsidis et al., 2023) where RH_i tends to exceed the RH_i threshold for homogeneous nucleation (implying that homogeneous ice nucleation is active near cloud top). These findings highlight a limitation in the treatment of pre-existing ice in climate models: in GCMs with coarse vertical resolutions (e.g., ~700 meters for cirrus clouds), the layer-mean ice mass mixing ratio (q_i) (used to predict ice nucleation in the presence of pre-existing ice) is often much higher than the actual q_i near cloud tops. This leads to an overestimation of pre-existing ice, which can bias the homogeneous and heterogeneous contributions and their radiative effects (Mitchell and Erfani, 2025; Mitchell and Garnier, 2024).

5.3 Physiscs and dynamics of cirrus clouds and mixed-phase clouds

Another important factor in cirrus cloud modeling is the role of dynamic processes such as orographic gravity waves (OGWs). OGWs are known to enhance ice nucleation in cirrus clouds by increasing their updrafts and supersaturations. Recent studies have demonstrated that including OGWs in GCMs leads to stronger homogeneous ice nucleation, and thereby higher N_i and IWC and lower D_e (Lyu et al., 2023; Tully et al., 2022). This suggests that GCMs should incorporate OGWs as a dynamic source for ice nucleation to better capture the microphysical and radiative

https://doi.org/10.5194/egusphere-2025-1165
Preprint. Discussion started: 25 March 2025

properties of cirrus clouds, but OGWs are currently missing in the National Center for Atmospheric Research (NCAR) GCMs (Lyu et al., 2023).

Furthermore, GCMs should account for complex processes for underlying mixed-phase clouds and their relationship with cirrus clouds. Through injecting INPs, CCT can modify cirrus cloud microphysics (e.g. reductions in N_i and increases in D_e) which then affects the growth processes of ice particles in mixed-phase clouds and causes more cooling due to CCT (Gruber et al., 2019; Mitchell et al., 2020). This realization helped give birth to a new climate intervention method known as mixed-phase regime cloud thinning or MCT (Villanueva et al., 2022). In the CCT investigation described in Mitchell et al. (2020) using the Whole Atmosphere Community Climate Model version 6 (WACCM6), most of the CCT CRE was due to mixed phase clouds that were affected by microphysical changes in the overlying cirrus clouds. This suggests that the glaciation of mixed phase clouds with subsequent CRE changes may be partly accomplished through CCT using INP concentrations on the order of 10 L^{-1} (Storelvmo et al., 2013; 2014) instead of the higher INP concentrations indicated in Villanueva et al. (2022), which were on the order of 10^5 L^{-1} in the Arctic for producing a CRE change of -1 W m^{-2}. This approach may also produce a CRE change or cooling effect greater than the CRE change produced by CCT or MCT alone.

A significant gap in CCT research is the lack of process-based modeling using high vertical and/or horizontal resolutions such as Large Eddy Simulations (LES) and single column models. To the best of our knowledge, only one LES study has been conducted on CCT (Gruber et al., 2019). This limits our understanding of smaller-scale processes such as turbulence, convection, and cloud physics in cirrus clouds. In contrast, extensive LES research has been employed for another SRM method, called marine cloud brightening (MCB), in order to resolve those processes (Chun et al., 2023; Erfani et al., 2022, 2024). The knowledge gained from such studies can then be employed to improve the representation of MCB in GCMs. Similar efforts are needed for understanding processes related to CCT. In particular, two of the afformentioned issues, pre-existing ice treatment and OGW parameterization, should not be significant in high-resolution LES experiments.

https://doi.org/10.5194/egusphere-2025-1165
Preprint. Discussion started: 25 March 2025

6 Conclusions

This study investigates CCT as a climate intervention method by quantifying it as the transition from homogeneous to heterogeneous cirrus clouds. Considering the challenges of achieving rapid GHG emission reductions, it has been argued that climate intervention methods may be necessary to mitigate global warming (Baiman et al., 2024; Kriegler et al., 2018). However, modifying the environment involves many risks, including unintended consequences for air quality, weather, and climate (Blackstock et al., 2009; Pereira et al., 2021). For this reason, it is important to conduct comprehensive research in order to quantify the efficacy, risks, costs, and limitations of such methods. Even if these methods pass all necessary tests, they are not alternatives to GHG emission reduction; rather, they are intended to "buy time" for societies to avoid the worst consequences of climate change until GHG emissions (and concentrations perhaps) are reduced to safe levels.

GCMs are advantageous for identifying the global net forcing of cirrus clouds, while accounting for climate feedback processes. However, inaccurate cirrus cloud processes (e.g., homogeneous and heterogeneous nucleation, and OGW cirrus) and unrealistic assumptions (e.g., pre-existing ice treatment) cause uncertainties in GCM simulations of CCT. For instance, GCMs that did not account for pre-existing ice predicted efficient CCT cooling (Storelvmo et al., 2013, 2014), while those that implemented pre-existing ice suggested minimal CCT effects (e.g., Gasparini and Lohmann, 2016). In contrast, process-based models, such as the RTM used in this study, can help isolate certain mechanisms and that knowledge can then be used to improve GCMs.

This study integrates the CALIPSO satellite retrievals described in Mitchell and Garnier (2024) with the libRadtran RTM to improve estimates of the radiative effects of homogeneous and heterogeneous cirrus clouds. Our results confirm that homogeneous cirrus clouds exert a significantly stronger CRE than heterogeneous cirrus, which implies that transitioning from homogeneous to heterogeneous cirrus, as a means of quantifying CCT, can result in substantial cooling, particularly in polar regions during winter. Our estimated surface cooling in the Polar Regions (which we call instantaneous CCT efficacy) ranges from -0.7 to -1.0 W m^{-2}, with a TOA cooling of -1.2 to -1.6 W m^{-2}. These values align with the cooling range of -0.25 to -2 W m^{-2} estimated by previous GCM studies (Gasparini et al., 2020; Gasparini and Lohmann, 2016; Storelvmo et al., 2013; Storelvmo and Herger, 2014; Storelvmo et al., 2014).

https://doi.org/10.5194/egusphere-2025-1165
Preprint. Discussion started: 25 March 2025

A major concern raised by previous CCT studies is *overseeding*, where injecting excessive INPs forms too many small ice particles through heterogeneous nucleation in cirrus clouds, leading to higher optical thickness, longer cloud lifetime, and ultimately a warming effect (Gasparini and Lohmann, 2016; Penner et al., 2015; Storelvmo et al., 2013; Tully et al., 2022). A related seeding concern is the creation of new cirrus clouds in clear sky regions where the RH_i is above ice saturation and natural INP concentrations are relatively low. By nature, RTMs cannot directly test these side effects or any other adjustment or feedback processes. However, regarding the latter, Gruber et al. (2019) investigated CCT for an Arctic case study using the ICON-ART modeling system with a horizontal resolution of 5 km and an integration time step of 25 s, and found that while seeding produced some new cirrus clouds, these new cirrus suppressed homogeneous nucleation downstream by lowering RH_i further downstream, with these two phenomena tending to cancel in terms of their radiative effect. And in regard to overseeding, this rarely occurred since homogeneous nucleation in natural cirrus was active throughout most of the model domain. Another concern is the potential impact of CCT on precipitation; however, this impact seems to be small as a change in cirrus CRE caused by CCT can lead to a global mean rainfall reduction of -1.3%, which is less than corresponding estimates for another climate engineering SRM method known as stratospheric aerosol injection (Storelvmo et al., 2014).

Over the mid-latitudes during winter, RTM simulations show that CCT cooling at the TOA and within the atmosphere is comparable to that in the polar regions. However, no significant impact is observed at the surface due to competing LW and SW radiation effects: homogeneous cirrus absorbs/emits more LW radiation but also scatters more SW radiation than heterogeneous cirrus and these two effects cancel each other. This finding is consistent with Storelvmo et al. (2014), who suggested that conducting CCT globally is not more efficient than targeting high-latitude regions.

Sensitivity analyses reveal that the cooling efficacy of CCT is significantly affected by atmospheric thermodynamic profiles and the presence of low clouds. TOA cooling is sensitive to surface temperature, while surface cooling is less sensitive to changes in atmospheric water vapor. These findings align with previous studies (Corti and Peter, 2009; Dupont and Haeffelin, 2008), which demonstrated that cirrus CRE at the TOA depends on the temperature contrast between the Earth's surface and the cloud, whereas the cirrus CRE at the surface is reduced by a more humid

https://doi.org/10.5194/egusphere-2025-1165
Preprint. Discussion started: 25 March 2025

atmosphere due to the absorption of downward LW radiation by water vapor. Furthermore, these results indicate that Arctic low clouds tend to strongly suppress the instantaneous efficacy of CCT by insulating the surface from the CCT atmospheric cooling. However, this strong atmospheric cooling suggests that CCT may still influence the surface through mixing and other feedback mechanisms over longer timescales, even in the presence of low clouds.

One important CCT operating principle not addressed in this study is the impact of changes in ice fall speed (V_i) (due to changes in D_e) on cloud lifetime and coverage. This principle is critical because it affects the temporal evolution of cirrus clouds, which our statistical, time-independent analysis cannot capture. In addition, the median D_e values for homogeneous and heterogeneous cirrus in our study were similar, and this is likely to cause an underestimation of the true D_e for heterogeneous cirrus if the D_e – IWC relationship is linear under pure heterogeneous conditions as illustrated in Fig. S5. Figure S5 is like Fig. S1 except that the linear portion of the D_e – IWC relationship (dominated by heterogeneous ice nucleation) is extrapolated to higher IWC values. Median D_e for these extrapolated relationships, presumably representative for pure heterogeneous nucleation conditions, would be larger than the heterogeneous D_e used in this study. Therefore, V_i would also be larger (Mishra et al., 2014), resulting in shorter cloud lifetimes and cloud fractions (Mitchell et al., 2008). By not accounting for this principle, our estimates of CCT CRE may be conservative. Future studies should incorporate time-dependent processes and explore the relationship between D_e, V_i, and cloud fraction to better quantify the efficacy of CCT.

Our study highlights the necessity of improving the representation of cirrus cloud processes in models, particularly the radiative contributions of the homogeneous and heterogeneous regimes. To more accurately quantify the efficacy of CCT, future work should focus on 1) using satellite retrievals of cirrus cloud properties to guide corresponding model parameterizations, 2) revisiting assumptions such as the treatment of pre-existing ice in GCMs, 3) including OGW cirrus clouds in GCMs, and 4) employing high-resolution LES experiments. While LES modeling has been widely used in studies of another climate intervention method (i.e., MCB), its application to CCT remains limited to a single study (e.g., Gruber et al., 2019). Considering the persistent uncertainties in observing and modeling aerosol-cloud-precipitation interactions related to cirrus clouds, an integration of spatially and temporally high-resolution in-situ and/or remote sensing measurements may be essential for constraining parameterizations and for improving the representation of ice

https://doi.org/10.5194/egusphere-2025-1165
Preprint. Discussion started: 25 March 2025

processes in LES and GCM modeling. In the future, we will incorporate CALIPSO retrievals of cirrus clouds in NCAR GCM, called Community Atmosphere Model, version 6 (CAM6) to quantify D_e as a function of IWC and T for different regions and seasons for a more accurate representation of CCT.

Data Availability Statement: The MERRA2 reanalysis data is publicly available at https://doi.org/10.5067/2E096JV59PK7 (Global Modeling and Assimilation Office (GMAO), 2015). The libRadtran code is publicly accessible at http://www.libradtran.org/doku.php (Emde et al., 2016). The CALIPSO retrievals of IWC and D_e from Mitchell and Garnier (2024), and the RTM outputs in this study will be provided upon request.

Competing interests: The authors declare that no competing interests are present.

Author contributions: All co-authors contributed to the conceptualization, methodology, and discussions about interpreting the results. EE developed the Python codes and conducted exploratory data analysis and RTM simulations. EE drafted the manuscript, and all co-authors provided edits and revisions.

Acknowledgments: This study was primarily supported by NOAA's Climate Program Office Earth's Radiation Budget (ERB) Program, Grant NA22OAR4690640. We appreciate Anne Garnier, Marco Giordano, John Mejia, Blaž Gasparini, and Claudia Emde for discussions on this research that contributed to the improvement of the final results.

https://doi.org/10.5194/egusphere-2025-1165
Preprint. Discussion started: 25 March 2025

References

Achtert, P., O'Connor, E. J., Brooks, I. M., Sotiropoulou, G., Shupe, M. D., Pospichal, B., Brooks, B. J., and Tjernström, M.: Properties of Arctic liquid and mixed-phase clouds from shipborne Cloudnet observations during ACSE 2014, Atmospheric Chemistry and Physics, 20, 14983–15002, https://doi.org/10.5194/acp-20-14983-2020, 2020.

Anderson, G. P., Clough, S. A., Kneizys, F., Chetwynd, J. H., and Shettle, E. P.: AFGL atmospheric constituent profiles (0.120 km), Air Force Geophysics Lab Hanscom AFB MA, 1986.

Baiman, R., Clarke, S., Elsworth, C., Field, L., MacCracken, M., Macdonald, J., Mitchell, D., Oeste, F. D., Reed, S., Salter, S., Simmens, H., Tao, Y., and Tulip, R.: Addressing the urgent need for direct climate cooling: Rationale and options, Oxford Open Climate Change, 4, kgae014, https://doi.org/10.1093/oxfclm/kgae014, 2024.

Baum, B. A., Yang, P., Heymsfield, A. J., Platnick, S., King, M. D., Hu, Y.-X., and Bedka, S. T.: Bulk Scattering Properties for the Remote Sensing of Ice Clouds. Part II: Narrowband Models, Journal of Applied Meteorology, 44, 1896–1911, https://doi.org/10.1175/JAM2309.1, 2005.

Bergstrom, R. W., Pilewskie, P., Russell, P. B., Redemann, J., Bond, T. C., Quinn, P. K., and Sierau, B.: Spectral absorption properties of atmospheric aerosols, Atmospheric Chemistry and Physics, 7, 5937–5943, https://doi.org/10.5194/acp-7-5937-2007, 2007.

Breider, T. J., Mickley, L. J., Jacob, D. J., Wang, Q., Fisher, J. A., Chang, Rachel. Y.-W., and Alexander, B.: Annual distributions and sources of Arctic aerosol components, aerosol optical depth, and aerosol absorption: Ann. dist. & sources of Arctic aerosol, J. Geophys. Res. Atmos., 119, 4107–4124, https://doi.org/10.1002/2013JD020996, 2014.

Buras, R., Dowling, T., and Emde, C.: New secondary-scattering correction in DISORT with increased efficiency for forward scattering, Journal of Quantitative Spectroscopy and Radiative Transfer, 112, 2028–2034, https://doi.org/10.1016/j.jqsrt.2011.03.019, 2011.

Chun, J.-Y., Wood, R., Blossey, P., and Doherty, S. J.: Microphysical, macrophysical, and radiative responses of subtropical marine clouds to aerosol injections, Atmospheric Chemistry and Physics, 23, 1345–1368, https://doi.org/10.5194/acp-23-1345-2023, 2023.

Cohen, J., Zhang, X., Francis, J., Jung, T., Kwok, R., Overland, J., Ballinger, T. J., Bhatt, U. S., Chen, H. W., Coumou, D., Feldstein, S., Gu, H., Handorf, D., Henderson, G., Ionita, M., Kretschmer, M., Laliberte, F., Lee, S., Linderholm, H. W., Maslowski, W., Peings, Y., Pfeiffer, K., Rigor, I., Semmler, T., Stroeve, J., Taylor, P. C., Vavrus, S., Vihma, T., Wang, S., Wendisch, M., Wu, Y., and Yoon, J.: Divergent consensuses on Arctic amplification influence on midlatitude severe winter weather, Nat. Clim. Chang., 10, 20–29, https://doi.org/10.1038/s41558-019-0662-y, 2020.

Córdoba-Jabonero, C., Gómez-Martín, L., del Águila, A., Vilaplana, J. M., López-Cayuela, M.-Á., and Zorzano, M.-P.: Cirrus-induced shortwave radiative effects depending on their optical and physical properties: Case studies using simulations and measurements, Atmospheric Research, 246, 105095, https://doi.org/10.1016/j.atmosres.2020.105095, 2020.

Corti, T. and Peter, T.: A simple model for cloud radiative forcing, Atmospheric Chemistry and Physics, 9, 5751–5758, https://doi.org/10.5194/acp-9-5751-2009, 2009.

Creamean, J. M., de Boer, G., Telg, H., Mei, F., Dexheimer, D., Shupe, M. D., Solomon, A., and McComiskey, A.: Assessing the vertical structure of Arctic aerosols using balloon-borne measurements, Atmospheric Chemistry and Physics, 21, 1737–1757, https://doi.org/10.5194/acp-21-1737-2021, 2021.

https://doi.org/10.5194/egusphere-2025-1165
Preprint. Discussion started: 25 March 2025

Cziczo, D. J., Froyd, K. D., Hoose, C., Jensen, E. J., Diao, M., Zondlo, M. A., Smith, J. B., Twohy, C. H., and Murphy, D. M.: Clarifying the Dominant Sources and Mechanisms of Cirrus Cloud Formation, Science, 340, 1320–1324, https://doi.org/10.1126/science.1234145, 2013.

Dagsson-Waldhauserova, P., Renard, J.-B., Olafsson, H., Vignelles, D., Berthet, G., Verdier, N., and Duverger, V.: Vertical distribution of aerosols in dust storms during the Arctic winter, Sci Rep, 9, 16122, https://doi.org/10.1038/s41598-019-51764-y, 2019.

Dekoutsidis, G., Groß, S., Wirth, M., Krämer, M., and Rolf, C.: Characteristics of supersaturation in midlatitude cirrus clouds and their adjacent cloud-free air, Atmospheric Chemistry and Physics, 23, 3103–3117, https://doi.org/10.5194/acp-23-3103-2023, 2023.

Dowling, D. R. and Radke, L. F.: A Summary of the Physical Properties of Cirrus Clouds, Journal of Applied Meteorology and Climatology, 29, 970–978, https://doi.org/10.1175/1520-0450(1990)029<0970:ASOTPP>2.0.CO;2, 1990.

Dupont, J.-C. and Haeffelin, M.: Observed instantaneous cirrus radiative effect on surface-level shortwave and longwave irradiances, Journal of Geophysical Research: Atmospheres, 113, https://doi.org/10.1029/2008JD009838, 2008.

Eastman, R. and Warren, S. G.: Interannual Variations of Arctic Cloud Types in Relation to Sea Ice, Journal of Climate, 23, 4216–4232, https://doi.org/10.1175/2010JCLI3492.1, 2010.

Eidhammer, T., Morrison, H., Mitchell, D., Gettelman, A., and Erfani, E.: Improvements in Global Climate Model Microphysics Using a Consistent Representation of Ice Particle Properties, https://doi.org/10.1175/JCLI-D-16-0050.1, 2017.

Eliasson, S., Buehler, S. A., Milz, M., Eriksson, P., and John, V. O.: Assessing observed and modelled spatial distributions of ice water path using satellite data, Atmospheric Chemistry and Physics, 11, 375–391, https://doi.org/10.5194/acp-11-375-2011, 2011.

Emde, C., Buras-Schnell, R., Kylling, A., Mayer, B., Gasteiger, J., Hamann, U., Kylling, J., Richter, B., Pause, C., Dowling, T., and Bugliaro, L.: The libRadtran software package for radiative transfer calculations (version 2.0.1), Geosci. Model Dev., 9, 1647–1672, https://doi.org/10.5194/gmd-9-1647-2016, 2016.

Erfani, E. and Mitchell, D. L.: Developing and bounding ice particle mass- and area-dimension expressions for use in atmospheric models and remote sensing, Atmos. Chem. Phys., 16, 4379–4400, https://doi.org/10.5194/acp-16-4379-2016, 2016.

Erfani, E. and Mitchell, D. L.: Growth of ice particle mass and projected area during riming, Atmospheric Chemistry and Physics, 17, 1241–1257, https://doi.org/10.5194/acp-17-1241-2017, 2017.

Erfani, E., Blossey, P., Wood, R., Mohrmann, J., Doherty, S. J., Wyant, M., and O, K.: Simulating Aerosol Lifecycle Impacts on the Subtropical Stratocumulus-to-Cumulus Transition Using Large-Eddy Simulations, Journal of Geophysical Research: Atmospheres, 127, e2022JD037258, https://doi.org/10.1029/2022JD037258, 2022.

Erfani, E., Wood, R., Blossey, P., Doherty, S. J., and Eastman, R.: Building a comprehensive library of observed Lagrangian trajectories for testing modeled cloud evolution, aerosol-cloud interactions, and marine cloud brightening, EGUsphere, 1–52, https://doi.org/10.5194/egusphere-2024-3232, 2024.

Evans, K. F., Wang, J. R., O'C Starr, D., Heymsfield, G., Li, L., Tian, L., Lawson, R. P., Heymsfield, A. J., and Bansemer, A.: Ice hydrometeor profile retrieval algorithm for high-frequency microwave radiometers: application to the CoSSIR instrument during TC4, Atmos. Meas. Tech., 5, 2277–2306, https://doi.org/10.5194/amt-5-2277-2012, 2012.

https://doi.org/10.5194/egusphere-2025-1165
Preprint. Discussion started: 25 March 2025

Fauchez, T., Davis, A. B., Cornet, C., Szczap, F., Platnick, S., Dubuisson, P., and Thieuleux, F.: A fast hybrid (3-D/1-D) model for thermal radiative transfer in cirrus via successive orders of scattering, Journal of Geophysical Research: Atmospheres, 122, 344–366, https://doi.org/10.1002/2016JD025607, 2017.

Forster, P., Storelvmo, T., Armour, K., Collins, W., Dufresne, J.-L., Frame, D., Lunt, D., Mauritsen, T., Palmer, M., and Watanabe, M.: The Earth's energy budget, climate feedbacks, and climate sensitivity, in: Climate Change 2021: The Physical Science Basis. Contribution of Working Group I to the Sixth Assessment Report of the Intergovernmental Panel on Climate Change [Masson-Delmotte, V., P. Zhai, A. Pirani, S. L. Connors, C. Péan, S. Berger, N. Caud, Y. Chen, L. Goldfarb, M. I. Gomis, M. Huang, K. Leitzell, E. Lonnoy, J.B.R. Matthews, T. K. Maycock, T. Waterfield, O. Yelekçi, R. Yu and B. Zhou (eds.)], Cambridge University Press, Cambridge, United Kingdom, 2021.

Froyd, K. D., Yu, P., Schill, G. P., Brock, C. A., Kupc, A., Williamson, C. J., Jensen, E. J., Ray, E., Rosenlof, K. H., Bian, H., Darmenov, A. S., Colarco, P. R., Diskin, G. S., Bui, T., and Murphy, D. M.: Dominant role of mineral dust in cirrus cloud formation revealed by global-scale measurements, Nat. Geosci., 15, 177–183, https://doi.org/10.1038/s41561-022-00901-w, 2022.

Fu, Q. and Liou, K. N.: Parameterization of the Radiative Properties of Cirrus Clouds, Journal of the Atmospheric Sciences, 50, 2008–2025, https://doi.org/10.1175/1520-0469(1993)050<2008:POTRPO>2.0.CO;2, 1993.

Gao, B.-C., Yang, P., Han, W., Li, R.-R., and Wiscombe, W. J.: An algorithm using visible and 1.38-/spl mu/m channels to retrieve cirrus cloud reflectances from aircraft and satellite data, IEEE Transactions on Geoscience and Remote Sensing, 40, 1659–1668, 2002.

Gasparini, B. and Lohmann, U.: Why cirrus cloud seeding cannot substantially cool the planet, J. Geophys. Res. Atmos., 121, 4877–4893, https://doi.org/10.1002/2015JD024666, 2016.

Gasparini, B., McGraw, Z., Storelvmo, T., and Lohmann, U.: To what extent can cirrus cloud seeding counteract global warming?, Environ. Res. Lett., 15, 054002, https://doi.org/10.1088/1748-9326/ab71a3, 2020.

Gasparini, B., Sullivan, S. C., Sokol, A. B., Kärcher, B., Jensen, E., and Hartmann, D. L.: Opinion: Tropical cirrus – from micro-scale processes to climate-scale impacts, Atmospheric Chemistry and Physics, 23, 15413–15444, https://doi.org/10.5194/acp-23-15413-2023, 2023.

Gasteiger, J., Emde, C., Mayer, B., Buras, R., Buehler, S. A., and Lemke, O.: Representative wavelengths absorption parameterization applied to satellite channels and spectral bands, Journal of Quantitative Spectroscopy and Radiative Transfer, 148, 99–115, https://doi.org/10.1016/j.jqsrt.2014.06.024, 2014.

Gelaro, R., McCarty, W., Suárez, M. J., Todling, R., Molod, A., and Takacs, L.: The modern-era retrospective analysis for research and applications, version 2 (MERRA-2), J. Clim., 30, 5419–5454, https://doi.org/10.1175/JCLI-D-16-0758.1, 2017.

Gettelman, A. and Morrison, H.: Advanced Two-Moment Bulk Microphysics for Global Models. Part I: Off-Line Tests and Comparison with Other Schemes, J. Clim., 28, 1268–1287, https://doi.org/10.1175/jcli-d-14-00102.1, 2015.

Global Modeling and Assimilation Office (GMAO): MERRA-2 inst3_3d_asm_Np: 3d,3-Hourly,Instantaneous,Pressure-Level,Assimilation,Assimilated Meteorological Fields V5.12.4, Greenbelt, MD, USA, Goddard Earth Sciences Data and Information Services Center (GES DISC)[Dataset], https://doi.org/10.5067/QBZ6MG944HW0, 2015c.

https://doi.org/10.5194/egusphere-2025-1165
Preprint. Discussion started: 25 March 2025

Gouveia, D. A., Barja, B., Barbosa, H. M. J., Seifert, P., Baars, H., Pauliquevis, T., and Artaxo, P.: Optical and geometrical properties of cirrus clouds in Amazonia derived from 1 year of ground-based lidar measurements, Atmospheric Chemistry and Physics, 17, 3619–3636, https://doi.org/10.5194/acp-17-3619-2017, 2017.

Groot Zwaaftink, C. D., Grythe, H., Skov, H., and Stohl, A.: Substantial contribution of northern high-latitude sources to mineral dust in the Arctic, Journal of Geophysical Research: Atmospheres, 121, 13,678-13,697, https://doi.org/10.1002/2016JD025482, 2016.

Gruber, S., Blahak, U., Haenel, F., Kottmeier, C., Leisner, T., Muskatel, H., Storelvmo, T., and Vogel, B.: A Process Study on Thinning of Arctic Winter Cirrus Clouds With High-Resolution ICON-ART Simulations, Journal of Geophysical Research: Atmospheres, 124, 5860–5888, https://doi.org/10.1029/2018JD029815, 2019.

Gryspeerdt, E., Sourdeval, O., Quaas, J., Delanoë, J., Krämer, M., and Kühne, P.: Ice crystal number concentration estimates from lidar–radar satellite remote sensing – Part 2: Controls on the ice crystal number concentration, Atmospheric Chemistry and Physics, 18, 14351–14370, https://doi.org/10.5194/acp-18-14351-2018, 2018.

Guignard, A., Stubenrauch, C. J., Baran, A. J., and Armante, R.: Bulk microphysical properties of semi-transparent cirrus from AIRS: a six year global climatology and statistical analysis in synergy with geometrical profiling data from CloudSat-CALIPSO, Atmos. Chem. Phys., 12, 503–525, https://doi.org/10.5194/acp-12-503-2012, 2012.

Hartmann, D. L.: Global physical climatology, 2nd ed., Elsevier Science, Amsterdam, 485 pp., 2016.

Heymsfield, A. J., Krämer, M., Luebke, A., Brown, P., Cziczo, D. J., Franklin, C., Lawson, P., Lohmann, U., McFarquhar, G., Ulanowski, Z., and Tricht, K. V.: Cirrus Clouds, Meteorological Monographs, 58, 2.1-2.26, https://doi.org/10.1175/AMSMONOGRAPHS-D-16-0010.1, 2017.

Hong, Y., Liu, G., and Li, J.-L. F.: Assessing the Radiative Effects of Global Ice Clouds Based on CloudSat and CALIPSO Measurements, Journal of Climate, 29, 7651–7674, https://doi.org/10.1175/JCLI-D-15-0799.1, 2016.

Hu, Y. X. and Stamnes, K.: An Accurate Parameterization of the Radiative Properties of Water Clouds Suitable for Use in Climate Models, Journal of Climate, 6, 728–742, https://doi.org/10.1175/1520-0442(1993)006<0728:AAPOTR>2.0.CO;2, 1993.

Huang, Y., Dong, X., Kay, J. E., Xi, B., and McIlhattan, E. A.: The climate response to increased cloud liquid water over the Arctic in CESM1: a sensitivity study of Wegener–Bergeron–Findeisen process, Clim Dyn, 56, 3373–3394, https://doi.org/10.1007/s00382-021-05648-5, 2021.

IPCC report: Technical summary, in: Climate Change 2021: The Physical Science Basis. Contribution of Working Group I to the Sixth Assessment Report of the Intergovernmental Panel on Climate Change, Cambridge University Press, Cambridge, United Kingdom and New York, NY, USA, 33–144, https://doi.org/10.1017/9781009157896.001, 2021.

Järvinen, E., Nehlert, F., Xu, G., Waitz, F., Mioche, G., Dupuy, R., Jourdan, O., and Schnaiter, M.: Investigating the vertical extent and short-wave radiative effects of the ice phase in Arctic summertime low-level clouds, Atmospheric Chemistry and Physics, 23, 7611–7633, https://doi.org/10.5194/acp-23-7611-2023, 2023.

Jiang, J. H., Yue, Q., Su, H., Kangaslahti, P., Lebsock, M., Reising, S., Schoeberl, M., Wu, L., and Herman, R. L.: Simulation of Remote Sensing of Clouds and Humidity From Space

https://doi.org/10.5194/egusphere-2025-1165
Preprint. Discussion started: 25 March 2025

Using a Combined Platform of Radar and Multifrequency Microwave Radiometers, Earth and Space Science, 6, 1234–1243, https://doi.org/10.1029/2019EA000580, 2019.

Kanji, Z. A., Ladino, L. A., Wex, H., Boose, Y., Burkert-Kohn, M., Cziczo, D. J., and Krämer, M.: Overview of Ice Nucleating Particles, https://doi.org/10.1175/AMSMONOGRAPHS-D-16-0006.1, 2017.

Kärcher, B.: Cirrus Clouds and Their Response to Anthropogenic Activities, Curr Clim Change Rep, 3, 45–57, https://doi.org/10.1007/s40641-017-0060-3, 2017.

Kay, J. E., Hillman, B. R., Klein, S. A., Zhang, Y., Medeiros, B., Pincus, R., Gettelman, A., Eaton, B., Boyle, J., and Marchand, R.: Exposing global cloud biases in the Community Atmosphere Model (CAM) using satellite observations and their corresponding instrument simulators, Journal of Climate, 25, 5190–5207, https://doi.org/10.1175/JCLI-D-11-00469.1, 2012.

Khvorostyanov, V. I. and Sassen, K.: Cirrus Cloud Simulation Using Explicit Microphysics and Radiation. Part I: Model Description, Journal of the Atmospheric Sciences, 55, 1808–1821, https://doi.org/10.1175/1520-0469(1998)055<1808:CCSUEM>2.0.CO;2, 1998.

Krämer, M., Rolf, C., Luebke, A., Afchine, A., Spelten, N., Costa, A., Meyer, J., Zöger, M., Smith, J., Herman, R. L., Buchholz, B., Ebert, V., Baumgardner, D., Borrmann, S., Klingebiel, M., and Avallone, L.: A microphysics guide to cirrus clouds – Part 1: Cirrus types, Atmos. Chem. Phys., 16, 3463–3483, https://doi.org/10.5194/acp-16-3463-2016, 2016.

Krämer, M., Rolf, C., Spelten, N., Afchine, A., Fahey, D., Jensen, E., Khaykin, S., Kuhn, T., Lawson, P., Lykov, A., Pan, L. L., Riese, M., Rollins, A., Stroh, F., Thornberry, T., Wolf, V., Woods, S., Spichtinger, P., Quaas, J., and Sourdeval, O.: A microphysics guide to cirrus – Part 2: Climatologies of clouds and humidity from observations, Atmospheric Chemistry and Physics, 20, 12569–12608, https://doi.org/10.5194/acp-20-12569-2020, 2020.

Kriegler, E., Luderer, G., Bauer, N., Baumstark, L., Fujimori, S., Popp, A., Rogelj, J., Strefler, J., and van Vuuren, D. P.: Pathways limiting warming to 1.5°C: a tale of turning around in no time?, Philosophical Transactions of the Royal Society A: Mathematical, Physical and Engineering Sciences, 376, 20160457, https://doi.org/10.1098/rsta.2016.0457, 2018.

Lawson, R. P., Woods, S., Jensen, E., Erfani, E., Gurganus, C., Gallagher, M., Connolly, P., Whiteway, J., Baran, A. J., May, P., Heymsfield, A., Schmitt, C. G., McFarquhar, G., Um, J., Protat, A., Bailey, M., Lance, S., Muehlbauer, A., Stith, J., Korolev, A., Toon, O. B., and Krämer, M.: A Review of Ice Particle Shapes in Cirrus formed In Situ and in Anvils, Journal of Geophysical Research: Atmospheres, 124, 10049–10090, https://doi.org/10.1029/2018JD030122, 2019.

Li, Q. and Groß, S.: Changes in cirrus cloud properties and occurrence over Europe during the COVID-19-caused air traffic reduction, Atmos. Chem. Phys., 21, 14573–14590, https://doi.org/10.5194/acp-21-14573-2021, 2021.

Loeb, N. G., Wielicki, B. A., Doelling, D. R., Smith, G. L., Keyes, D. F., Kato, S., Manalo-Smith, N., and Wong, T.: Toward Optimal Closure of the Earth's Top-of-Atmosphere Radiation Budget, Journal of Climate, 22, 748–766, https://doi.org/10.1175/2008JCLI2637.1, 2009.

Lyu, K., Liu, X., Bacmeister, J., Zhao, X., Lin, L., Shi, Y., and Sourdeval, O.: Orographic Cirrus and Its Radiative Forcing in NCAR CAM6, Journal of Geophysical Research: Atmospheres, 128, e2022JD038164, https://doi.org/10.1029/2022JD038164, 2023.

Macke, A., Francis, P. N., McFarquhar, G. M., and Kinne, S.: The Role of Ice Particle Shapes and Size Distributions in the Single Scattering Properties of Cirrus Clouds, Journal of the

Atmospheric Sciences, 55, 2874–2883, https://doi.org/10.1175/1520-0469(1998)055<2874:TROIPS>2.0.CO;2, 1998.

Magurno, D., Cossich, W., Maestri, T., Bantges, R., Brindley, H., Fox, S., Harlow, C., Murray, J., Pickering, J., Warwick, L., and Oetjen, H.: Cirrus Cloud Identification from Airborne Far-Infrared and Mid-Infrared Spectra, Remote Sensing, 12, 2097, https://doi.org/10.3390/rs12132097, 2020.

Maillard, J., Ravetta, F., Raut, J.-C., Mariage, V., and Pelon, J.: Characterisation and surface radiative impact of Arctic low clouds from the IAOOS field experiment, Atmos. Chem. Phys., 21, 4079–4101, https://doi.org/10.5194/acp-21-4079-2021, 2021.

Marsing, A., Meerkötter, R., Heller, R., Kaufmann, S., Jurkat-Witschas, T., Krämer, M., Rolf, C., and Voigt, C.: Investigating the radiative effect of Arctic cirrus measured in situ during the winter 2015–2016, Atmospheric Chemistry and Physics, 23, 587–609, https://doi.org/10.5194/acp-23-587-2023, 2023.

Matus, A. V. and L'Ecuyer, T. S.: The role of cloud phase in Earth's radiation budget: CLOUD PHASE IN EARTH'S RADIATION BUDGET, J. Geophys. Res. Atmos., 122, 2559–2578, https://doi.org/10.1002/2016JD025951, 2017.

Mishra, S., Mitchell, D. L., Turner, D. D., and Lawson, R. P.: Parameterization of ice fall speeds in midlatitude cirrus: Results from SPartICus, J. Geophys. Res.-Atmos., 119, 3857–3876, https://doi.org/10.1002/2013jd020602, 2014.

Mitchell, D. L. and Erfani, E.: Cirrus Cloud Thinning, in: Geoengineering and Climate Change, John Wiley & Sons, Ltd, 297–306, https://doi.org/10.1002/9781394204847.ch18, 2025.

Mitchell, D. L. and Finnegan, W.: Modification of cirrus clouds to reduce global warming, Environ. Res. Lett., 4, 045102, https://doi.org/10.1088/1748-9326/4/4/045102, 2009.

Mitchell, D. L. and Garnier, A.: Advances in CALIPSO (IIR) cirrus cloud property retrievals. Part 2: Global estimates of the fraction of cirrus clouds affected by homogeneous ice nucleation, https://doi.org/10.5194/egusphere-2024-3814, 12 December 2024.

Mitchell, D. L., Rasch, P., Ivanova, D., McFarquhar, G., and Nousiainen, T.: Impact of small ice crystal assumptions on ice sedimentation rates in cirrus clouds and GCM simulations, Geophys. Res. Lett., 35, L09806, https://doi.org/10.1029/2008gl033552, 2008.

Mitchell, D. L., Garnier, A., Pelon, J., and Erfani, E.: CALIPSO (IIR–CALIOP) retrievals of cirrus cloud ice-particle concentrations, Atmospheric Chemistry and Physics, 18, 17325–17354, https://doi.org/10.5194/acp-18-17325-2018, 2018.

Mitchell, D. L., Mejia, J., Garnier, A., Tomii, Y., Krämer, M., and Hosseinpour, F.: An Estimate of Global, Regional and Seasonal Cirrus Cloud Radiative Effects Contributed by Homogeneous Ice Nucleation, Atmospheric Chemistry and Physics Discussions, 1–48, https://doi.org/10.5194/acp-2020-846, 2020.

Mitchell, D. L., Garnier, A. E., and Woods, S.: Advances in CALIPSO (IIR) cirrus cloud property retrievals – Part 1: Methods and testing, EGUsphere, 1–44, https://doi.org/10.5194/egusphere-2024-3790, 2024.

Monroe, E. E., Taylor, P. C., and Boisvert, L. N.: Arctic Cloud Response to a Perturbation in Sea Ice Concentration: The North Water Polynya, JGR Atmospheres, 126, https://doi.org/10.1029/2020JD034409, 2021.

Moschos, V., Dzepina, K., Bhattu, D., Lamkaddam, H., Casotto, R., Daellenbach, K. R., Canonaco, F., Rai, P., Aas, W., Becagli, S., Calzolai, G., Eleftheriadis, K., Moffett, C. E., Schnelle-Kreis, J., Severi, M., Sharma, S., Skov, H., Vestenius, M., Zhang, W., Hakola, H., Hellén, H., Huang, L., Jaffrezo, J.-L., Massling, A., Nøjgaard, J. K., Petäjä, T., Popovicheva,

https://doi.org/10.5194/egusphere-2025-1165
Preprint. Discussion started: 25 March 2025

O., Sheesley, R. J., Traversi, R., Yttri, K. E., Schmale, J., Prévôt, A. S. H., Baltensperger, U., and El Haddad, I.: Equal abundance of summertime natural and wintertime anthropogenic Arctic organic aerosols, Nat. Geosci., 15, 196–202, https://doi.org/10.1038/s41561-021-00891-1, 2022.

NASEM report: Reflecting Sunlight: Recommendations for Solar Geoengineering Research and Research Governance, The national academies press, Washington, D.C., https://doi.org/10.17226/25762, 2021.

Nazaryan, H., McCormick, M. P., and Menzel, W. P.: Global characterization of cirrus clouds using CALIPSO data, J. Geophys. Res., 113, D16211, https://doi.org/10.1029/2007JD009481, 2008.

Penner, J. E., Zhou, C., and Liu, X.: Can cirrus cloud seeding be used for geoengineering?, Geophysical Research Letters, 42, 8775–8782, https://doi.org/10.1002/2015GL065992, 2015.

Pereira, L., Morrow, D., Aquila, V., Beckage, B., Beckbesinger, S., Beukes, L., Buck, H., Carlson, C., Geden, O., Jones, A., Keller, D., Mach, K., Mashigo, M., Moreno-Cruz, J., Visioni, D., Nicholson, S., and Trisos, C.: From fAIrplay to climate wars: making climate change scenarios more dynamic, creative, and integrative, Ecology and Society, 26, https://doi.org/10.5751/ES-12856-260430, 2021.

Philipp, D., Stengel, M., and Ahrens, B.: Analyzing the Arctic Feedback Mechanism between Sea Ice and Low-Level Clouds Using 34 Years of Satellite Observations, Journal of Climate, 33, 7479–7501, https://doi.org/10.1175/JCLI-D-19-0895.1, 2020.

Roskovensky, J. K. and Liou, K. N.: Detection of thin cirrus from 1.38 μm/0.65 μm reflectance ratio combined with 8.6–11 μm brightness temperature difference, Geophysical Research Letters, 30, https://doi.org/10.1029/2003GL018135, 2003.

Samset, B. H., Stjern, C. W., Andrews, E., Kahn, R. A., Myhre, G., Schulz, M., and Schuster, G. L.: Aerosol Absorption: Progress Towards Global and Regional Constraints, Curr Clim Change Rep, 4, 65–83, https://doi.org/10.1007/s40641-018-0091-4, 2018.

Sassen, K., Wang, Z., and Liu, D.: Cirrus clouds and deep convection in the tropics: Insights from CALIPSO and CloudSat, J. Geophys. Res., 114, D00H06, https://doi.org/10.1029/2009JD011916, 2009.

Schläpfer, D., Richter, R., and Reinartz, P.: Elevation-Dependent Removal of Cirrus Clouds in Satellite Imagery, Remote Sensing, 12, 494, https://doi.org/10.3390/rs12030494, 2020.

Schmale, J., Sharma, S., Decesari, S., Pernov, J., Massling, A., Hansson, H.-C., von Salzen, K., Skov, H., Andrews, E., Quinn, P. K., Upchurch, L. M., Eleftheriadis, K., Traversi, R., Gilardoni, S., Mazzola, M., Laing, J., and Hopke, P.: Pan-Arctic seasonal cycles and long-term trends of aerosol properties from 10 observatories, Atmos. Chem. Phys., 22, 3067–3096, https://doi.org/10.5194/acp-22-3067-2022, 2022.

Schumann, U., Mayer, B., Graf, K., and Mannstein, H.: A Parametric Radiative Forcing Model for Contrail Cirrus, Journal of Applied Meteorology and Climatology, 51, 1391–1406, https://doi.org/10.1175/JAMC-D-11-0242.1, 2012.

Screen, J. A. and Simmonds, I.: The central role of diminishing sea ice in recent Arctic temperature amplification, Nature, 464, 1334–1337, https://doi.org/10.1038/nature09051, 2010.

Shettle, E. P.: Models of aerosols, clouds, and precipitation for atmospheric propagation studies, in: In AGARD Conference Proceedings, ADS Bibcode: 1990apuv.agar.....S, 1989.

Shi, X., Liu, X., and Zhang, K.: Effects of pre-existing ice crystals on cirrus clouds and comparison between different ice nucleation parameterizations with the Community

https://doi.org/10.5194/egusphere-2025-1165
Preprint. Discussion started: 25 March 2025

Atmosphere Model (CAM5), Atmospheric Chemistry and Physics, 15, 1503–1520, https://doi.org/10.5194/acp-15-1503-2015, 2015.

Sourdeval, O., Gryspeerdt, E., Krämer, M., Goren, T., Delanoë, J., Afchine, A., Hemmer, F., and Quaas, J.: Ice crystal number concentration estimates from lidar–radar satellite remote sensing – Part 1: Method and evaluation, Atmospheric Chemistry and Physics, 18, 14327–14350, https://doi.org/10.5194/acp-18-14327-2018, 2018.

Stamnes, K., Tsay, S.-C., Wiscombe, W., and Laszlo, I.: DISORT, a general-purpose Fortran program for discrete-ordinate-method radiative transfer in scattering and emitting layered media: documentation of methodology, 2000.

Steffen, W., Rockström, J., Richardson, K., Lenton, T. M., Folke, C., Liverman, D., Summerhayes, C. P., Barnosky, A. D., Cornell, S. E., Crucifix, M., Donges, J. F., Fetzer, I., Lade, S. J., Scheffer, M., Winkelmann, R., and Schellnhuber, H. J.: Trajectories of the Earth System in the Anthropocene, Proceedings of the National Academy of Sciences, 115, 8252–8259, https://doi.org/10.1073/pnas.1810141115, 2018.

Stephens, G. L., Tsay, S.-C., Stackhouse, P. W., and Flatau, P. J.: The Relevance of the Microphysical and Radiative Properties of Cirrus Clouds to Climate and Climatic Feedback, 1990.

Storelvmo, T. and Herger, N.: Cirrus cloud susceptibility to the injection of ice nuclei in the upper troposphere, Journal of Geophysical Research: Atmospheres, 119, 2375–2389, https://doi.org/10.1002/2013JD020816, 2014.

Storelvmo, T., Kristjansson, J. E., Muri, H., Pfeffer, M., Barahona, D., and Nenes, A.: Cirrus cloud seeding has potential to cool climate, Geophysical Research Letters, 40, 178–182, https://doi.org/10.1029/2012GL054201, 2013.

Storelvmo, T., Boos, W. R., and Herger, N.: Cirrus cloud seeding: a climate engineering mechanism with reduced side effects?, Philosophical Transactions of the Royal Society A: Mathematical, Physical and Engineering Sciences, 372, 20140116, https://doi.org/10.1098/rsta.2014.0116, 2014.

Stubenrauch, C. J., Chédin, A., Rädel, G., Scott, N. A., and Serrar, S.: Cloud Properties and Their Seasonal and Diurnal Variability from TOVS Path-B, Journal of Climate, 19, 5531–5553, https://doi.org/10.1175/JCLI3929.1, 2006.

Stubenrauch, C. J., Cros, S., Lamquin, N., Armante, R., Chédin, A., Crevoisier, C., and Scott, N. A.: Cloud properties from Atmospheric Infrared Sounder and evaluation with Cloud-Aerosol Lidar and Infrared Pathfinder Satellite Observations, J. Geophys. Res., 113, D00A10, https://doi.org/10.1029/2008JD009928, 2008.

Sun, W., Videen, G., Kato, S., Lin, B., Lukashin, C., and Hu, Y.: A study of subvisual clouds and their radiation effect with a synergy of CERES, MODIS, CALIPSO, and AIRS data, Journal of Geophysical Research: Atmospheres, 116, https://doi.org/10.1029/2011JD016422, 2011.

Sun, Z.: Reply to comments by Greg M. McFarquhar on 'Parametrization of effective sizes of cirrus-cloud particles and its verification against observations'. (October B, 1999,125, 3037–3055), Q.J Royal Met. Soc., 127, 267–271, https://doi.org/10.1002/qj.49712757116, 2001.

Sun, Z. and Rikus, L.: Parametrization of effective sizes of cirrus-cloud particles and its verification against observations, Quarterly Journal of the Royal Meteorological Society, 125, 3037–3055, https://doi.org/10.1002/qj.49712556012, 1999.

https://doi.org/10.5194/egusphere-2025-1165
Preprint. Discussion started: 25 March 2025

Takano, Y., Liou, K. N., and Minnis, P.: The Effects of Small Ice Crystals on Cirrus Infrared Radiative Properties, Journal of the Atmospheric Sciences, 49, 1487–1493, https://doi.org/10.1175/1520-0469(1992)049<1487:TEOSIC>2.0.CO;2, 1992.

Tierney, J. E., King, J., Osman, M. B., Abell, J. T., Burls, N. J., Erfani, E., Cooper, V. T., and Feng, R.: Pliocene Warmth and Patterns of Climate Change Inferred From Paleoclimate Data Assimilation, AGU Advances, 6, e2024AV001356, https://doi.org/10.1029/2024AV001356, 2025.

Tully, C., Neubauer, D., Omanovic, N., and Lohmann, U.: Cirrus cloud thinning using a more physically based ice microphysics scheme in the ECHAM-HAM general circulation model, Atmos. Chem. Phys., 22, 11455–11484, https://doi.org/10.5194/acp-22-11455-2022, 2022.

Villanueva, D., Possner, A., Neubauer, D., Gasparini, B., Lohmann, U., and Tesche, M.: Mixed-phase regime cloud thinning could help restore sea ice, Environ. Res. Lett., 17, 114057, https://doi.org/10.1088/1748-9326/aca16d, 2022.

Wang, J., Liu, C., Yao, B., Min, M., Letu, H., Yin, Y., and Yung, Y. L.: A multilayer cloud detection algorithm for the Suomi-NPP Visible Infrared Imager Radiometer Suite (VIIRS), Remote Sensing of Environment, 227, 1–11, https://doi.org/10.1016/j.rse.2019.02.024, 2019.

Wang, J. R., Liu, G., Spinhirne, J. D., Racette, P., and Hart, W. D.: Observations and retrievals of cirrus cloud parameters using multichannel millimeter-wave radiometric measurements, J. Geophys. Res., 106, 15251–15263, https://doi.org/10.1029/2000JD900262, 2001.

Wilber, A. C., Kratz, D. P., and Gupta, S. K.: Surface Emissivity Maps for Use in Satellite Retrievals of Longwave Radiation, NASA Scientific and Technical Information, 1999.

Wolf, K., Bellouin, N., and Boucher, O.: Radiative effect by cirrus cloud and contrails – A comprehensive sensitivity study, Radiation/Atmospheric Modelling/Troposphere/Physics (physical properties and processes), https://doi.org/10.5194/egusphere-2023-155, 2023.

Wu, D. L., Lambert, A., Read, W. G., Eriksson, P., and Gong, J.: MLS and CALIOP Cloud Ice Measurements in the Upper Troposphere: A Constraint from Microwave on Cloud Microphysics, Journal of Applied Meteorology and Climatology, 53, 157–165, https://doi.org/10.1175/JAMC-D-13-041.1, 2014.

Xie, H., Wang, Z., Luo, T., Yang, K., Zhang, D., Zhou, T., Yang, X., Liu, X., and Fu, Q.: Seasonal Variation of Dust Aerosol Vertical Distribution in Arctic Based on Polarized Micropulse Lidar Measurement, Remote Sensing, 14, 5581, https://doi.org/10.3390/rs14215581, 2022.

Yorks, J. E., Wang, J., McGill, M. J., Follette-Cook, M., Nowottnick, E. P., Reid, J. S., Colarco, P. R., Zhang, J., Kalashnikova, O., Yu, H., Marenco, F., Santanello, J. A., Weckwerth, T. M., Li, Z., Campbell, J. R., Yang, P., Diao, M., Noel, V., Meyer, K. G., Carr, J. L., Garay, M., Christian, K., Bennedetti, A., Ring, A. M., Crawford, A., Pavolonis, M. J., Aquila, V., Kim, J., and Kondragunta, S.: A SmallSat Concept to Resolve Diurnal and Vertical Variations of Aerosols, Clouds, and Boundary Layer Height, Bulletin of the American Meteorological Society, https://doi.org/10.1175/BAMS-D-21-0179.1, 2023.

Yu, Y., Taylor, P. C., and Cai, M.: Seasonal Variations of Arctic Low-Level Clouds and Its Linkage to Sea Ice Seasonal Variations, Journal of Geophysical Research: Atmospheres, 124, 12206–12226, https://doi.org/10.1029/2019JD031014, 2019.

Yue, Q., Jiang, J. H., Heymsfield, A., Liou, K., Gu, Y., and Sinha, A.: Combining In Situ and Satellite Observations to Understand the Vertical Structure of Tropical Anvil Cloud Microphysical Properties During the TC4 Experiment, Earth and Space Science, 7, https://doi.org/10.1029/2020EA001147, 2020.

https://doi.org/10.5194/egusphere-2025-1165
Preprint. Discussion started: 25 March 2025

Zamora, L. M., Kahn, R. A., Cubison, M. J., Diskin, G. S., Jimenez, J. L., Kondo, Y., McFarquhar, G. M., Nenes, A., Thornhill, K. L., Wisthaler, A., Zelenyuk, A., and Ziemba, L. D.: Aircraft-measured indirect cloud effects from biomass burning smoke in the Arctic and subarctic, Atmospheric Chemistry and Physics, 16, 715–738, https://doi.org/10.5194/acp-16-715-2016, 2016.

Zhang, Y., Macke, A., and Albers, F.: Effect of crystal size spectrum and crystal shape on stratiform cirrus radiative forcing, Atmospheric Research, 52, 59–75, https://doi.org/10.1016/S0169-8095(99)00026-5, 1999.

Zhou, Y., Sun, X., Zhang, R., Zhang, C., Li, H., Zhou, J., and Li, S.: Influences of cloud heterogeneity on cirrus optical properties retrieved from the visible and near-infrared channels of MODIS/SEVIRI for flat and optically thick cirrus clouds, Journal of Quantitative Spectroscopy and Radiative Transfer, 187, 232–246, https://doi.org/10.1016/j.jqsrt.2016.09.020, 2017.

Zhu, X., Wang, Z., Liu, D., and Cai, H.: The First Global Insight of Cirrus Clouds Characterized by Hollow Ice Crystals From Space-Borne Lidar, Geophysical Research Letters, 51, e2024GL109852, https://doi.org/10.1029/2024GL109852, 2024.